



Cardiovascular Predictive Value and Genetic Basis of Ventricular Repolarization Dynamics

BACKGROUND: Early prediction of cardiovascular risk in the general population remains an important issue. The T-wave morphology restitution (TMR), an ECG marker quantifying ventricular repolarization dynamics, is strongly associated with cardiovascular mortality in patients with heart failure. Our aim was to evaluate the cardiovascular prognostic value of TMR in a UK middle-aged population and identify any genetic contribution.

METHODS: We analyzed ECG recordings from 55 222 individuals from a UK middle-aged population undergoing an exercise stress test in UK Biobank (UKB). TMR was used to measure ventricular repolarization dynamics, exposed in this cohort by exercise (TMR during exercise, TMR^{ex}) and recovery from exercise (TMR during recovery, TMR^{rec}). The primary end point was cardiovascular events; secondary end points were all-cause mortality, ventricular arrhythmias, and atrial fibrillation with median follow-up of 7 years. Genome-wide association studies for TMR^{ex} and TMR^{rec} were performed, and genetic risk scores were derived and tested for association in independent samples from the full UKB cohort (N=360 631).

RESULTS: A total of 1743 (3.2%) individuals in UKB who underwent the exercise stress test had a cardiovascular event, and TMR^{rec} was significantly associated with cardiovascular events (hazard ratio, 1.11; $P=5\times 10^{-7}$), independent of clinical variables and other ECG markers. TMR^{rec} was also associated with all-cause mortality (hazard ratio, 1.10) and ventricular arrhythmias (hazard ratio, 1.16). We identified 12 genetic loci in total for TMR^{ex} and TMR^{rec}, of which 9 are associated with another ECG marker. Individuals in the top 20% of the TMR^{rec} genetic risk score were significantly more likely to have a cardiovascular event in the full UKB cohort (18 997, 5.3%) than individuals in the bottom 20% (hazard ratio, 1.07; $P=6\times 10^{-3}$).

CONCLUSIONS: TMR and TMR genetic risk scores are significantly associated with cardiovascular risk in a UK middle-aged population, supporting the hypothesis that increased spatio-temporal heterogeneity of ventricular repolarization is a substrate for cardiovascular risk and the validity of TMR as a cardiovascular risk predictor.

VISUAL OVERVIEW: A [visual overview](#) is available for this article.

Julia Ramírez, PhD
Stefan van Duijvenboden, PhD
Nay Aung, MD, PhD
Pablo Laguna, PhD
Esther Pueyo, PhD
Andrew Tinker, MD, PhD*
Pier D. Lambiase, MD, PhD*
Michele Orini, PhD*
Patricia B. Munroe, PhD*

*Drs Tinker, Lambiase, Orini, and Munroe contributed equally as joint supervisors.

Key Words: exercise ■ genetic analyses ■ genetic risk score ■ middle aged ■ risk ■ T-wave morphology

© 2019 The Authors. *Circulation: Arrhythmia and Electrophysiology* is published on behalf of the American Heart Association, Inc., by Wolters Kluwer Health, Inc. This is an open access article under the terms of the [Creative Commons Attribution License](#), which permits use, distribution, and reproduction in any medium, provided that the original work is properly cited.

<https://www.ahajournals.org/journal/circep>



WHAT IS KNOWN?

- The T-wave morphology restitution (TMR) is a recently proposed ECG marker that quantifies the rate of variation of the T-wave morphology with heart rate.
- TMR is a strong predictor of sudden cardiac death in chronic heart failure patients.

WHAT THE STUDY ADDS?

- TMR at 1-minute recovery from exercise (TMR during recovery) was associated with cardiovascular risk (hazard ratio, 1.11; $P=5\times 10^{-7}$), all-cause mortality (hazard ratio, 1.10), and ventricular arrhythmic risk (hazard ratio 1.16) independent of clinical variables, resting corrected QT interval, and resting and recovery heart rate from an analysis of 60 000 individuals from a UK middle-aged population participating in an exercise stress test.
- Genetic loci for TMR during exercise and TMR during recovery were identified, of which 9 had been previously associated with other ECG markers. Individuals having a cardiovascular event in a $\approx 500\,000$ cohort had a higher genetic risk score for TMR during recovery than unaffected individuals.
- We demonstrate that TMR is a heritable risk marker for cardiovascular risk in a UK middle-aged population.

Cardiovascular mortality is the main cause of death in the general population,¹ and it accounts for 31% of all deaths worldwide, with its estimated cost expected to be \$1044 billion by 2030. Despite technological advances, prediction remains a critically important challenge.

The QT interval is the most recognized ECG index and reflects the duration of ventricular depolarization and repolarization. However, increasing evidence suggests that dispersion of repolarization and, in particular, its variations with heart rate, is a stronger marker for cardiovascular risk than the total duration of repolarization.^{2,3} The T-wave morphology restitution (TMR)⁴ is a recently proposed ECG marker that quantifies the rate of variation of the T-wave morphology with heart rate. This marker has shown to be a strong predictor of sudden cardiac death in chronic heart failure patients.^{4,5} However, its performance as a potential cardiovascular risk marker in the general population has not been evaluated. Furthermore, the biological mechanisms underlying TMR are not known.

ECG markers are heritable⁶ and statistical genetic methods are available to estimate the cumulative contribution of genetic factors to cardiovascular events via genetic risk scores (GRSs).⁷ We hypothesize that the interaction between repolarization dynamics and cardiovascular risk has a genetic component and that TMR can be used to capture it.

Our primary objective was to validate the prognostic significance of TMR in a dataset of 55 222 individuals where exercise and recovery from exercise were used to expose spatio-temporal heterogeneity of ventricular repolarization. Our secondary objectives were to perform genome-wide association studies (GWASs) to identify single-nucleotide variants (SNVs) determining the genetic contribution of TMR and to develop GRSs to evaluate their association with cardiovascular events in an independent population of 360 631 individuals.

METHODS

Anonymized data and materials have been returned to UK Biobank (UKB) and can be accessed per request.

Study Population, Follow-Up, and End Points

UKB is a prospective study of 488 377 individuals (FULL-UKB cohort), comprising relatively even numbers of men and women aged 40 to 69 years old at recruitment (2006–2008). A total of 95 216 individuals were invited for an exercise test using a stationary bicycle in conjunction with a 1-lead ECG device (Methods in the [Data Supplement](#)). Complete ECG recordings from 58 839 individuals, who were considered fit to perform the exercise stress test (EST), were available (EST in UKB [EST-UKB] cohort; Figure 1). Individuals were excluded if they had existing medical conditions known to affect heart rate, if they had experienced a previous cardiovascular event (matching the codes from Table I in the [Data Supplement](#)), if they were on heart rate altering medications, had been diagnosed with bundle branch block, if the ECG had poor quality, or there was no heart rate change during the exercise test (Methods in the [Data Supplement](#)). This led to $N=55\,222$ individuals included in the analyses. The UKB study has approval from the North West Multi-Centre Research Ethics Committee, and all participants provided informed consent.⁸

The primary end point of this study was cardiovascular events, defined as cardiovascular mortality or admission to hospital with a cardiovascular diagnosis. The exact *International Classification of Diseases, Tenth Revision* codes used to define cardiovascular events are presented in Table I in the [Data Supplement](#). The secondary end points were all-cause mortality (excluding external causes), ventricular arrhythmic events (defined as arrhythmic mortality or admission to hospital with an arrhythmic diagnosis), and atrial fibrillation. Details on cause and date of death and diagnoses are available in the Methods in the [Data Supplement](#). Follow-up was from the study inclusion date until March 31, 2017.

Derivation of TMR During Exercise and TMR During Recovery

The bicycle ergometer exercise test followed a standardized protocol: 15 s resting period, 2 minutes of constant load, 4 minutes of exercise during which the workload was gradually increased, and a 1-minute recovery period without pedaling (Figure 2A). Details of the preprocessing of

the ECG recordings are available in the Methods in the [Data Supplement](#). Automatic quantification of TMR during exercise (TMR^{ex}) and recovery (TMR^{rec}; shown in Figure 2) was performed on every ECG recording in 3 steps:

1. Derivation of average T waves: signal averaging of all available heartbeats within a 15 s window at rest, peak exercise, and recovery was used to reduce noise (Figure 2B). The onset, peak, and offset timings of the waveforms were located using bespoke software.^{9,10} Average T waves at rest, peak exercise, and recovery were selected using the T onset and T offset timings and were further low-pass filtered at 20 Hz.
2. T-wave morphology differences quantification: using a previously published algorithm based on time warping,¹¹ we derived the marker dw^{ex} , representing the average temporal stretching necessary to align each point of the average T wave at rest to the average T wave at peak exercise.¹¹ Figure 2C shows an example where 2 T waves have similar morphology and small dw^{ex} . Similarly, the marker dw^{rec} represents the average temporal stretching necessary to align each point of the average T wave at peak exercise and the average T wave at recovery. Figure 2C shows that the morphological difference between the 2 T waves has increased along with dw^{rec} .
3. TMR calculations: TMR^{ex} and TMR^{rec} were calculated by dividing dw^{ex} and dw^{rec} by the change in the RR interval (inverse of heart rate) during exercise, ΔRR^{ex} , and during recovery, ΔRR^{rec} , respectively, and represent the T-wave morphological change per RR increment during exercise and recovery, respectively.⁴

Computation of Other ECG markers

The QT interval and QRS duration were measured as the interval between the QRS-onset and the T-wave end, and between the QRS-onset and the QRS-offset, respectively, from the averaged heartbeat at rest. Then, we corrected the QT interval using Bazett formula.¹² We additionally derived the marker T-wave inversion, which indicated a change in the polarity of the T waves between resting and exercise stages¹³ (Methods in the [Data Supplement](#)).

Statistical Analyses

The 2-tailed Mann-Whitney and Fisher exact tests were used for univariate comparison of quantitative and categorical data, respectively. Correlation was evaluated with Spearman correlation coefficient. Receiver operator curves were derived using the pROC package¹⁴ from R and C-indices were calculated for each marker. We estimated the optimal cutoff values for TMR^{ex} and TMR^{rec} in a training set (N=27612) from the EST-UKB cohort (Methods in the [Data Supplement](#)) by means of log-rank statistics optimization with the aim of maximizing the predictive value. Kaplan-Meier curves were derived using the optimal cutoff values in the test set (N=27610), with a comparison of cumulative events performed by using log-rank tests.

Univariate and multivariate Cox regression analyses were performed to determine the predictive value of the risk markers. The proportional hazard assumptions were checked when applying these analyses. Continuous variables were

standardized to a mean of 0 and SD of 1 to allow for comparisons in the Cox models. Only the variables with a significant association with the end point in univariate analysis were included in the multivariate model. Individuals who died from causes not included in the primary end point were censored at the time of death. A value of $P < 0.05$ was considered statistically significant. Statistical analyses were performed using R version 3.5.1.

Heritability and GWASs

Inverse-normal transformation of TMR^{ex} and TMR^{rec} was performed as the distributions were skewed and did not approximate a normal distribution (Figure 1 in the [Data Supplement](#)). Heritability was estimated using a variance components method (BOLT-REML).¹⁵ GWAS for TMR^{ex} and TMR^{rec} were performed in a discovery (N=29393) and replication (N=22382) datasets separately using a linear mixed model method (BOLT-LMM).¹⁶ The TMR^{ex} model included the following covariates: sex, age, body mass index (BMI), resting RR, ΔRR^{ex} and a binary indicator variable for the genotyping array (UKB versus UK BiLEVE). The TMR^{rec} model included covariates sex, age, BMI, recovery RR, ΔRR^{rec} and the genotyping array. After careful review of significant ($P < 1 \times 10^{-6}$) SNVs from the discovery GWASs, 6 variants for TMR^{ex} and 7 variants for TMR^{rec} were taken forward into replication. Replication was confirmed if the SNVs remained significant (with Bonferroni correction) and with concordant direction of effects to the discovery analyses. A full dataset GWAS for both TMR^{ex} and TMR^{rec} was conducted and additional loci reaching genome-wide significance ($P < 5 \times 10^{-8}$) were reported. Since TMR^{ex} and TMR^{rec} were genetically correlated ($\rho = 0.58$), multitrait analysis of GWAS¹⁷ was used to leverage additional loci discovery. Detailed information can be found in Methods in the [Data Supplement](#).

To examine if there were independent secondary SNVs at TMR loci, we applied genome-wide complex trait analysis¹⁸ for all reported loci from the full dataset GWAS. The percent variance of TMR^{ex} and TMR^{rec} explained by the identified loci was calculated with standard methods, detailed in the Methods in the [Data Supplement](#). Bioinformatics analyses were performed to annotate SNVs and identify candidate genes, including Variant Effect Predictor,¹⁹ GTEx (the Genotype-Tissue Expression project), and long-range chromatin interaction data.²⁰ We used PhenoScanner,²¹ GWAS catalog (<https://www.ebi.ac.uk/gwas/>), and UKBiobank ICD PheWeb (<http://pheweb.sph.umich.edu/SAIGE-UKB/>) to determine SNV and gene associations with other traits. Pathway analyses were performed using g:profiler.²² Further description of bioinformatics analyses can be found in the Methods in the [Data Supplement](#). We downloaded the summary statistics for atrial fibrillation²³ to calculate its genetic correlation with TMR^{ex} and TMR^{rec} using LD score regression.²⁴

Genetic Risk Score Analyses

We used PRSice v2²⁵ to construct the GRS for TMR^{ex} and TMR^{rec} using the effect sizes from the full-cohort GWASs (EST-UKB) and performed prediction for the primary end point in the full UKB cohort (FULL-UKB) dataset (after exclusions, Figure II and Methods in the [Data Supplement](#)). We

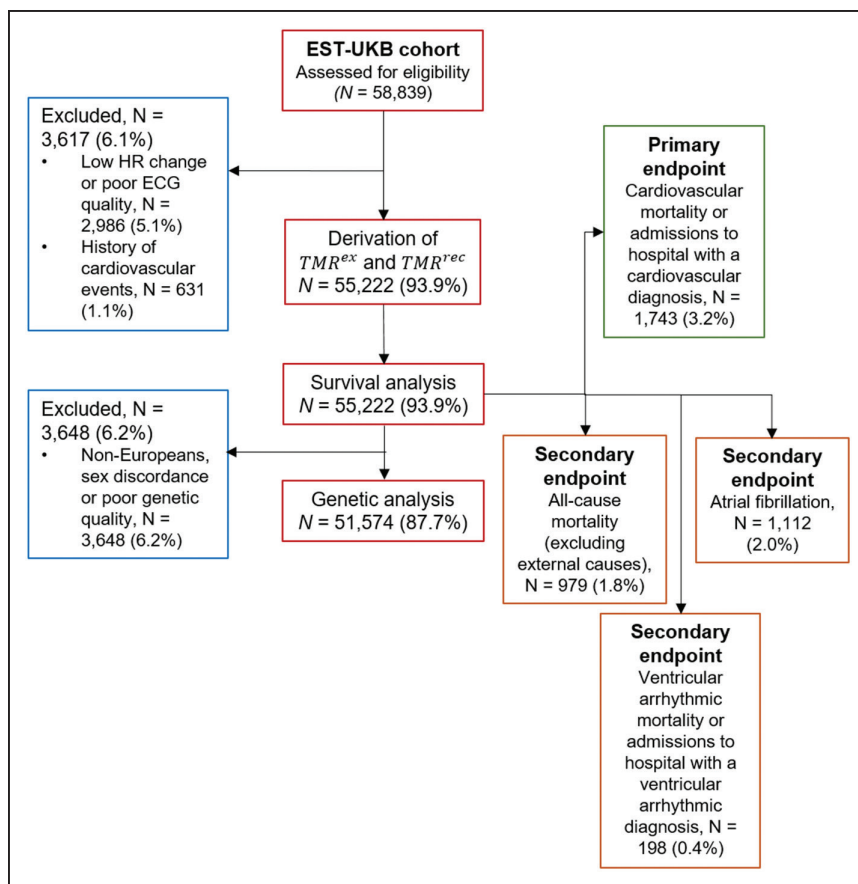


Figure 1. Flow diagram of analyses in the exercise stress test (EST; EST in UK Biobank [EST-UKB]) population. HR indicates heart rate; TMR, T-wave morphology restitution; TMR^{ex}, TMR during exercise; and TMR^{rec}, TMR during recovery.

first removed individuals included in the GWASs (EST-UKB) and their relatives, then removed all individuals with a previous history of cardiovascular events and non-Europeans. The GRSs were standardized to have a mean of 0 and an SD of 1. Their association with the study end points was tested in the FULL-UKB cohort (after exclusions, Figure II in the [Data Supplement](#)) using Mann-Whitney and Univariate Cox regression analyses.

RESULTS

Predictive Value of TMR in a UK Middle-Aged Population

The EST-UKB population consisted of 55222 individuals (25669 males, 29553 females) aged 40 to 73 years (mean 57 ± 8 years) after exclusions. The demographic characteristics of this population are shown in Table II in the [Data Supplement](#). During the follow-up, 1743 (3.2%) individuals had a cardiovascular event. The distributions of TMR^{ex} and TMR^{rec} are shown in Figure I in the [Data Supplement](#).

Age, BMI, TMR^{rec} ($P < 2 \times 10^{-16}$ for all), TMR^{ex} ($P = 3 \times 10^{-8}$) and resting heart rate ($P = 3 \times 10^{-4}$) were significantly higher in the cardiovascular events group than in the event-free group, whereas heart rate response to exercise and recovery were lower

($P < 2 \times 10^{-16}$ for both). Also, there were more males, diabetics, hypertensives (stage 1 [$130 \text{ mm Hg} \leq \text{systolic blood pressure} < 140 \text{ mm Hg}$ or $85 \text{ mm Hg} \leq \text{diastolic blood pressure} < 90 \text{ mm Hg}$] and stage 2 [$\text{systolic blood pressure} \geq 140 \text{ mm Hg}$ or $\text{diastolic blood pressure} \geq 90 \text{ mm Hg}$]), individuals with high cholesterol levels ($P < 2 \times 10^{-16}$ for all), smokers ($P = 1 \times 10^{-13}$), diagnosed with chronic kidney disease ($P = 5 \times 10^{-2}$), or with T-wave inversions ($P = 9 \times 10^{-3}$). QRS duration was not significantly different in individuals with and without cardiovascular events and thus was not included in the survival analyses (Table III and Figure III in the [Data Supplement](#)). Spearman correlation coefficient between TMR^{ex} and TMR^{rec} was 0.484; lower correlations were found between them and covariates (Table IV in the [Data Supplement](#)).

Individuals in the TMR^{ex} ≥ 0.082 group (stratified according to the optimal cutoff value—Figure IV in the [Data Supplement](#)) had 1.65 fold risk (95% CI, 1.38–1.98) of having a cardiovascular event than those in the TMR^{ex} < 0.082 group ($P < 10^{-3}$; Figure 3A). Similarly, individuals in the TMR^{rec} ≥ 0.115 group (Figure V in the [Data Supplement](#)) had 1.71 fold risk (95% CI, 1.43–2.05) of having a cardiovascular event than those in the TMR^{rec} < 0.115 groups ($P < 10^{-3}$; Figure 3B).

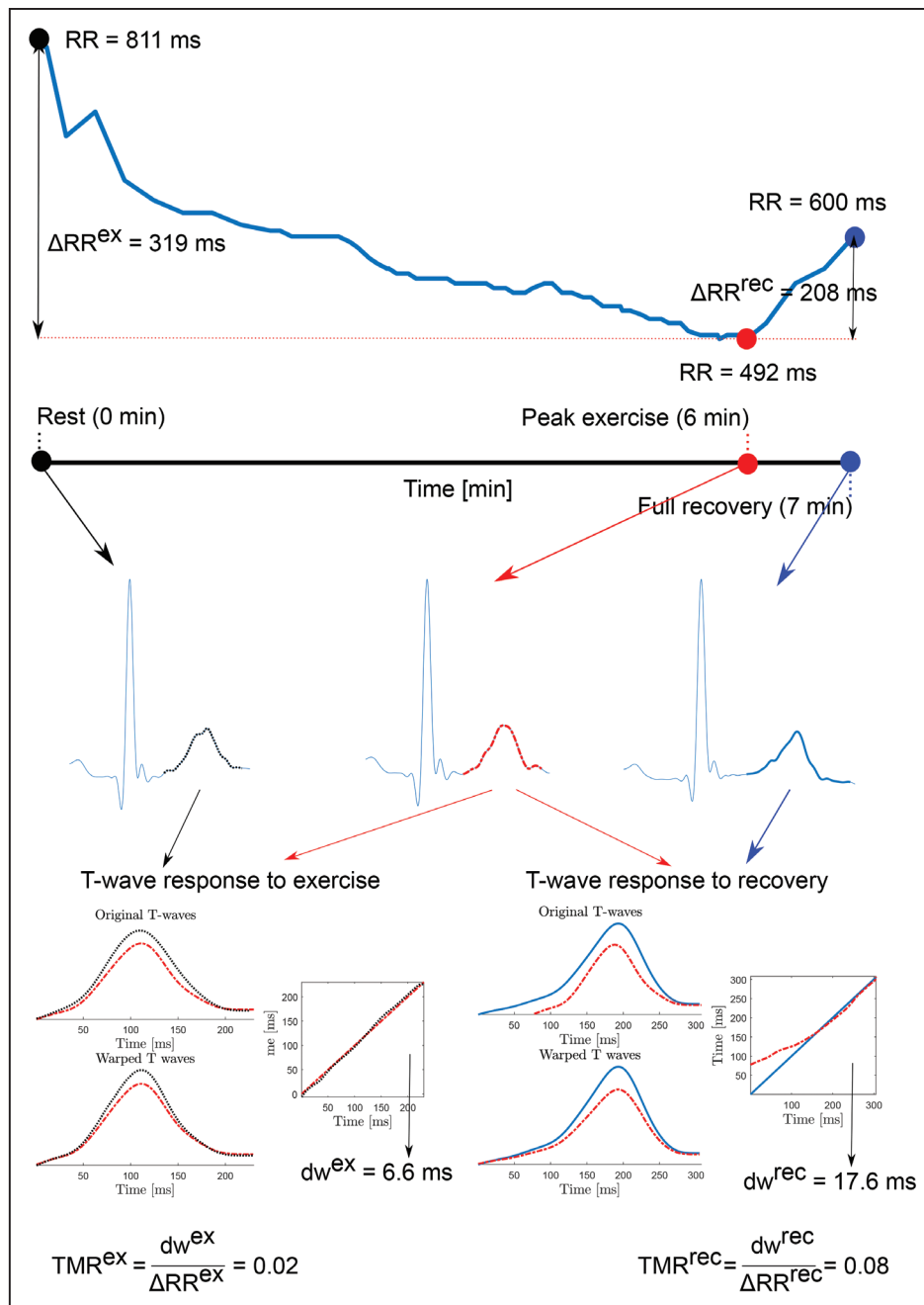


Figure 2. Assessment of T-wave morphology restitution (TMR).

A, Illustration of the RR profile during the exercise stress test. **B**, Three averaged heartbeats are derived at rest (black), peak exercise (red) and 50 s after peak exercise (full recovery, blue), respectively. **C**, TMR during exercise (TMR^{ex}) and TMR during recovery (TMR^{rec}) are derived by quantifying the morphological change between the T waves at rest (black T wave) and at peak exercise (red T wave), and between the T waves at peak exercise and full recovery (blue T wave), respectively, normalized by the corresponding RR change. ΔRR^{ex} indicates change in RR interval during exercise; and ΔRR^{rec} , change in RR interval during recovery.

To compare the hazard ratios (HRs) of TMR^{ex} and TMR^{rec} with those from other continuous markers, independently from cutoff thresholds, we included the continuous TMR^{ex} and TMR^{rec} markers into a multivariate Cox regression model. The following variables remained significantly associated with cardiovascular events (HR [95% CI] reported): chronic kidney disease (2.85 [1.07–7.62]), sex (2.82 [2.52–3.15]), T-wave inversion (2.21 [1.10–4.45]), age (1.73 [1.63–1.84]),

diabetes mellitus (1.56 [1.32–1.84]), hypertension stage 2 (1.32 [1.15–1.51]), hypertension stage 1 (1.19 [1.02–1.39]), BMI (1.18 [1.13–1.25]), corrected QT interval (1.11 [1.06–1.17]), and TMR^{rec} (1.11 [1.07–1.16]; Table 1). Among ECG markers, resting heart rate, heart rate responses to exercise and recovery, and TMR^{ex} were no longer significant. Among all cardiovascular events, 81.7% were related to ischemic heart disease. TMR^{rec} was independently associated

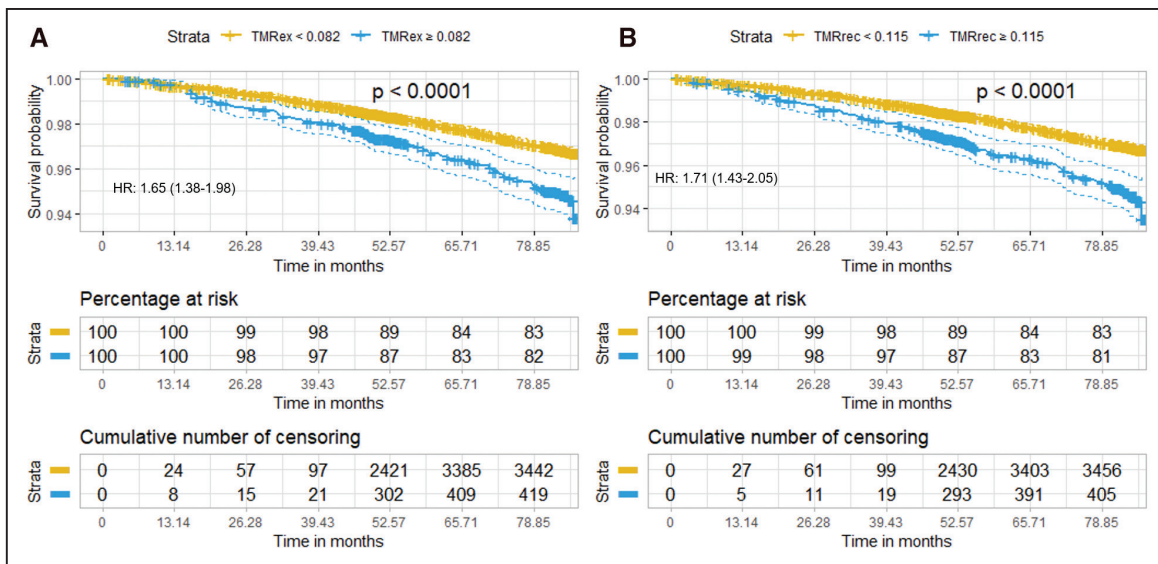


Figure 3. Kaplan-Meier survival curves. Cumulative survival rates of individuals stratified by T-wave morphology restitution (TMR) during exercise (TMR^{ex}) of ≥0.082 (A) and by TMR during recovery (TMR^{rec}) of ≥0.115 (B). Dashed lines indicate the 95% confidence levels. HR indicates hazard ratio.

with both ischemic (HR [95% CI] of 1.08 [1.03–1.13]) and nonischemic (HR [95% CI] of 1.20 [1.11–1.30]) causes (Tables VA and VB in the [Data Supplement](#)). The assumption of proportional hazards was supported for all covariates.

For the secondary end points, there were 979 (1.8%) cases of all-cause mortality, 198 (0.4%) who had a ventricular arrhythmic event, and 1112 (2.0%) who had atrial fibrillation (Table II in the [Data Supplement](#)). In multivariate Cox analysis, TMR^{rec} remained significantly associated

Table 1. Association With Cardiovascular Risk

	Univariate		Multivariate	
	HR (95% CI)	P Value	HR (95% CI)	P Value
Clinical variables				
Age (per 1 SD)	1.88 (1.78–2.00)	<2×10 ⁻¹⁶ *	1.73 (1.63–1.84)	<2×10 ⁻¹⁶ *
Sex (male)	3.01 (2.70–3.35)	<2×10 ⁻¹⁶ *	2.82 (2.52–3.15)	<2×10 ⁻¹⁶ *
Diabetes mellitus (yes)	2.71 (2.31–3.19)	<2×10 ⁻¹⁶ *	1.56 (1.32–1.84)	2.20×10 ⁻⁷ *
High cholesterol (yes)	1.95 (1.72–2.20)	<2×10 ⁻¹⁶ *	1.10 (0.97–1.25)	1.60×10 ⁻¹
BMI (per 1 SD)	1.28 (1.23–1.34)	<2×10 ⁻¹⁶ *	1.18 (1.13–1.25)	3.00×10 ⁻¹¹ *
Hypertensive stage 1	1.72 (1.48–2.01)	4.10×10 ⁻¹² *	1.19 (1.02–1.39)	2.60×10 ⁻² *
Hypertensive stage 2	2.43 (2.14–2.76)	<2×10 ⁻¹⁶ *	1.32 (1.15–1.51)	4.70×10 ⁻⁵ *
Previous or current smoker (yes)	1.38 (1.25–1.53)	9.30×10 ⁻¹¹ *	1.10 (0.99–1.21)	8.60×10 ⁻²
CKD (yes)	3.62 (1.36–9.66)	1.00×10 ⁻² *	2.85 (1.07–7.62)	3.70×10 ⁻² *
ECG variables				
Resting heart rate (per 1 SD)	1.10 (1.05–1.15)	5.70×10 ⁻⁵ *	0.97 (0.91–1.03)	2.90×10 ⁻¹
Heart rate response to exercise (per 1 SD)	0.70 (0.66–0.74)	<2×10 ⁻¹⁶ *	1.02 (0.94–1.10)	6.70×10 ⁻¹
Heart rate response to recovery (per 1 SD)	0.74 (0.71–0.76)	<2×10 ⁻¹⁶ *	0.96 (0.90–1.03)	2.50×10 ⁻¹
Corrected QT (per 1 SD)	1.15 (1.10–1.20)	4.00×10 ⁻¹⁰ *	1.11 (1.06–1.17)	5.40×10 ⁻⁵ *
T-wave inversion (yes)	2.80 (1.40–5.60)	3.70×10 ⁻³ *	2.21 (1.10–4.45)	2.70×10 ⁻² *
TMR during exercise (per 1 SD)	1.17 (1.12–1.22)	6.10×10 ⁻¹⁵ *	1.03 (0.98–1.08)	2.50×10 ⁻¹
TMR during recovery (per 1 SD)	1.23 (1.19–1.28)	<2×10 ⁻¹⁶ *	1.11 (1.07–1.16)	4.90×10 ⁻⁷ *

Hypertensive stage 1 defined as 130 mm Hg ≤ SBP <140 mm Hg or 85 mm Hg ≤ DBP <90 mm Hg. Hypertensive stage 2 defined as SBP ≥140 mm Hg or DBP ≥90 mm Hg. Reference Hypertension group is Hypertensive stage 0, defined as SBP <130 mm Hg and DBP <85 mm Hg. BMI indicates body mass index; CKD, chronic kidney disease; DBP, diastolic blood pressure; HR, hazard ratio; SBP, systolic blood pressure; and TMR, T-wave morphology restitution.

*Indicates statistically significant.

Table 2. Loci Associated With TMR During Exercise

Locus	SNV	CHR	BP	EA	EAF	Discovery			Replication			Combined					
						P Value	N	β	SE	P Value	N	β	SE	P Value	N	β	SE
RNF207§	rs709208	1	6272137	A	0.679	2.60×10 ⁻⁷	27 939	-0.042	0.008	1.60×10 ⁻⁵	20 769	-0.040	0.009	1.80×10 ⁻¹¹	49 203	-0.041	0.006
NOS1AP*†	rs12143842	1	162033890	C	0.750	1.20×10 ⁻⁴	29 393	-0.033	0.008	3.40×10 ⁻³	21 850	-0.029	0.010	6.60×10 ⁻⁷	51 764	-0.032	0.006
SCN5A-SCN10A*‡	rs7428232	3	38778618	T	0.416	5.20×10 ⁻⁶	29 352	-0.034	0.007	1.80×10 ⁻⁴	21 820	-0.032	0.008	3.70×10 ⁻⁹	51 692	-0.033	0.006
PREP	rs4478445	6	105786660	C	0.943	2.50×10 ⁻⁵	28 913	-0.067	0.016	7.40×10 ⁻³	21 493	-0.049	0.018	8.00×10 ⁻⁷	50 919	-0.059	0.012
KCNH2	rs2072412	7	150647970	C	0.729	1.80×10 ⁻⁶	28 975	0.040	0.008	4.10×10 ⁻⁷	21 539	0.048	0.010	2.10×10 ⁻¹¹	51 028	0.042	0.006
KCNQ1*§	rs2074238	11	2484803	T	0.088	1.10×10 ⁻⁸	29 393	-0.073	0.013	1.20×10 ⁻³	21 850	-0.048	0.015	1.20×10 ⁻¹	51 764	-0.062	0.010
SOX5*§	rs7307613	12	24595192	C	0.505	1.80×10 ⁻⁷	29 359	0.038	0.007	3.50×10 ⁻⁶	21 825	0.039	0.008	2.80×10 ⁻¹²	51 704	0.039	0.006
KCNJ2§	17:68493468_GA_G	17	68493468	GA	0.674	7.60×10 ⁻⁷	29 318	0.039	0.008	3.70×10 ⁻⁷	21 794	0.046	0.009	2.90×10 ⁻¹³	51 632	0.043	0.006

The locus name indicates the gene that is in the closest proximity to the most associated SNV. BP indicates position, based on human genome build 19; CHR, chromosome; EA, effect allele; EAF, effect allele frequency from discovery data; LD, linkage disequilibrium; MTAG, multitrait analysis of genome-wide association study; N, number of participants; SNV, single-nucleotide variation; and TMR, T-wave morphology restitution.

*SNV is the same or in high LD (r²>0.8) with an SNV associated with the other index.
 †Identified with MTAG.
 ‡Has a secondary signal.
 §Replicated SNVs.

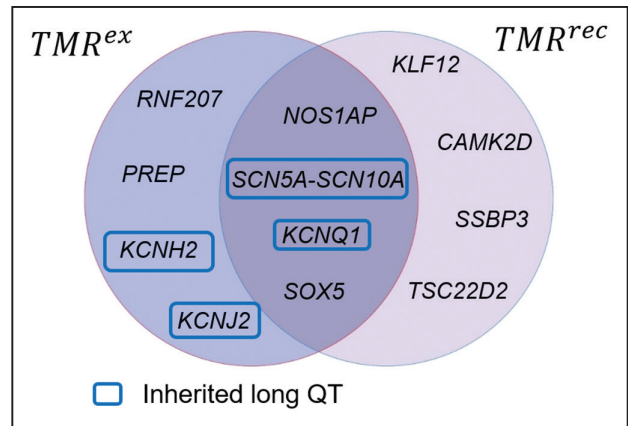


Figure 4. Overlap of loci for T-wave morphology restitution (TMR) during exercise (TMR^{ex}) and TMR during recovery (TMR^{rec}). The loci names indicate the coding gene that is in the closest proximity to the most associated single-nucleotide variation.

with all-cause mortality (HR [95% CI] of 1.10 [1.04–1.17]) independently of age, sex, smoke, diabetes mellitus, resting heart rate, heart rate response to recovery, and heart rate response to exercise (Table VI in the [Data Supplement](#)). TMR^{rec} also remained significantly associated with ventricular arrhythmic events (HR [95% CI] of 1.16 [1.03–1.30]) independently of sex, age, and heart rate response to recovery (Table VII in the [Data Supplement](#)). Finally, TMR^{rec} was not independently associated with atrial fibrillation (Table VIII in the [Data Supplement](#)).

Twelve Genetic Loci Are Associated With TMR

A total of 51 574 subjects were taken forward for genetic analyses after applying genetic quality control and excluding individuals of non-European ancestry (Figure 1). The heritability estimations of TMR^{ex} and TMR^{rec} were 3.5% and 4.9%, respectively, and their phenotypic correlation was 0.43.

In the discovery cohort GWAS (Methods), 1 genome-wide significant ($P \leq 5 \times 10^{-8}$) locus was found for TMR^{ex}, and 3 for TMR^{rec} (Table IX in the [Data Supplement](#)). Four SNVs for TMR^{ex} and 3 for TMR^{rec} formally replicated in the independent validation cohort (Tables 2 and 3). In the full dataset analysis, 2 additional SNVs reached genome-wide significance for TMR^{ex} and 4 SNVs for TMR^{rec}, respectively, all with concordant directions of effect (Tables 2 and 3). Manhattan plots for the full dataset are shown in Figure VI in the [Data Supplement](#). Visual inspection of the corresponding QQ plots from the discovery and full dataset GWASs did not show evidence of *P* value inflation or confounding (Figure VII in the [Data Supplement](#)). Analysis using multitrait analysis of GWAS¹⁷ (Methods) indicated 2 additional loci were significantly associated with TMR^{ex} and 1 for TMR^{rec} (Tables XA and XB in the [Data Supplement](#)). Sex-stratified analyses did not identify sex-specific loci for TMR^{ex}

Table 3. Loci Associated With TMR During Recovery

Locus	SNV	CHR	BP	EA	EAF	Discovery			Replication			Combined					
						P Value	N	β	SE	P Value	N	β	SE	P Value	N	β	SE
<i>SSBP3</i>	rs562408	1	54742618	A	0.430	6.20×10 ⁻⁶	28299	0.030	0.007	7.40×10 ⁻³	21091	0.020	0.008	3.70×10 ⁻⁸	49895	0.027	0.005
<i>NOS1AP</i> §	rs12143842	1	162033890	C	0.750	8.10×10 ⁻⁹	29013	-0.043	0.007	1.60×10 ⁻⁸	21623	-0.048	0.009	5.10×10 ⁻¹⁶	51153	-0.045	0.006
<i>SCN5A-SCN10A</i> **	rs7373065	3	38710315	T	0.019	2.00×10 ⁻⁶	26979	0.114	0.024	2.10×10 ⁻⁶	20107	0.132	0.028	1.60×10 ⁻¹¹	47566	0.122	0.018
<i>TSC22D2</i>	rs112717154	3	149943115	G	0.863	1.40×10 ⁻⁶	27857	-0.046	0.010	5.30×10 ⁻³	20762	-0.031	0.011	9.30×10 ⁻⁹	49115	-0.041	0.007
<i>CAIMK2D</i>	rs35408611	4	114423677	C	0.738	6.20×10 ⁻³	28362	-0.020	0.007	1.40×10 ⁻⁸	21138	-0.048	0.008	2.90×10 ⁻⁸	50006	-0.031	0.006
<i>KCNQ1</i> *§	rs2074238	11	2484803	T	0.088	1.40×10 ⁻³¹	29013	-0.131	0.011	4.20×10 ⁻³¹	21623	-0.152	0.013	1.20×10 ⁻⁵⁹	51153	-0.138	0.008
<i>SOX5</i> *§	rs1396206	12	24576859	A	0.482	3.10×10 ⁻¹³	28318	0.048	0.007	4.00×10 ⁻⁵	21105	0.031	0.007	1.30×10 ⁻¹⁶	49927	0.040	0.005
<i>KLF12</i> †	rs7992314	13	74509346	G	0.631	2.50×10 ⁻⁶	28908	-0.032	0.007	6.00×10 ⁻³	21545	-0.021	0.008	6.40×10 ⁻⁸	50968	-0.027	0.005

The locus name indicates the gene that is in the closest proximity to the most associated SNV. BP indicates position, based on human genome build 19; CHR, chromosome; EA, effect allele; EAF, effect allele frequency from discovery data; LD, linkage disequilibrium; MTAG, multitrait analysis of genome-wide association study; N, number of participants; SNV, single-nucleotide variation; and TMR, T-wave morphology restitution.

*SNV is the same or in high LD ($r^2>0.8$) with an SNV associated with the other index.
 †Identified with MTAG.
 ‡Has a secondary signal.
 §Replicated SNVs.

or TMR^{rec}. Conditional analyses showed evidence for 2 secondary independent signals at the *SCN5A-SCN10A* locus, 1 for each trait (Tables 2 and 3).

In total, 12 loci were identified, 8 for each trait with SNVs at 4 loci associated with both markers (Figure 4). The lead SNVs at the shared loci at *NOS1AP*, *KCNQ1*, *SCN5A-SCN10A*, and *SOX5* were identical or in high linkage disequilibrium ($r^2>0.8$). The identified SNVs for TMR^{ex} explained 0.63% of its variance. Similarly, the 8 SNVs identified for TMR^{rec} explained 1.14% of its variance. This corresponds to 20% and 23% of the estimated heritability for each TMR marker, respectively.

Variants at 7 of the 12 TMR loci have previously been reported to be associated with resting QT (*RNF207*, *KCNH2*, *KCNJ2*, *NOS1AP*, *SCN5A-SCN10A*, *KCNQ1*, and *KLF12*). Regional plots are shown in Figure VIII in the [Data Supplement](#). Look-ups in PhenoScanner indicated 9 of the 12 SNVs have associations with other cardiovascular markers, including pulse rate, QT interval, PR interval, QRS duration, P-wave duration, cardiac arrhythmias, and heart function (Tables XIA and XIB in the [Data Supplement](#)).

None of the lead variants or their close proxies ($r^2>0.8$) were annotated as missense variants. Variants at 2 loci *NOS1AP* and *SSBP3* were associated with expression levels of nearby genes (*c1orf226* and *SSBP3*, respectively) in heart atrial appendage samples (Table XII in the [Data Supplement](#)). We found 11 potential target genes whose promoter regions form significant chromatin interactions at 9 TMR loci (Table XIII in the [Data Supplement](#)). Using this information and literature review, we derived a list of candidate genes at each locus (Table XIV in the [Data Supplement](#)).

Table XV in the [Data Supplement](#) shows a lookup of all candidate genes in the GWAS catalog and in UKBio-bank ICD PheWeb and indicate associations across different cardiovascular traits, including atrial fibrillation. Our LD Score regression analysis indicated there was no significant genetic correlation between TMR^{ex} or TMR^{rec} and atrial fibrillation. The top 3 biological pathways for TMR^{ex} were cardiac muscle cell action potential ($P=4\times 10^{-10}$), regulation of ventricular cardiac muscle cell membrane repolarization ($P=4.7\times 10^{-10}$), and ventricular cardiac muscle cell membrane repolarization ($P=1\times 10^{-9}$; Figure IX in the [Data Supplement](#)). The analyses for TMR^{rec} indicated similar pathways including cardiac muscle cell action potential ($P=6.6\times 10^{-8}$), regulation of cardiac muscle contraction ($P=1.2\times 10^{-7}$), and regulation of striated muscle contraction ($P=3\times 10^{-7}$, Figure X in the [Data Supplement](#)).

Predictive Value of GRSs for TMR

After excluding individuals from the EST-UKB cohort and applying the exclusion criteria defined in Methods, the FULL-UKB population consisted of 360631 healthy

individuals (160 793 men, 199 838 women) aged 40 to 73 years (mean 57 ± 8 years, Figure II and Table II in the [Data Supplement](#)). During the follow-up, 18 997 (5.3%) individuals had a cardiovascular event, and 12 081 (3.3%), 2040 (0.6%) and 14 517 (4.0%) were individuals of all-cause mortality, ventricular arrhythmic events, and atrial fibrillation, respectively.

The optimal GRS for TMR^{ex} was derived combining 3442 SNVs identified using a P value of 3.1×10^{-3} for thresholding (Figure XI in the [Data Supplement](#)). This GRS was not significantly different between individuals with a cardiovascular event and those without ($P=5.5 \times 10^{-2}$). The optimal GRS for TMR^{rec} was derived combining 3281 SNVs with a $P < 2.9 \times 10^{-3}$ (Figure XII in the [Data Supplement](#)). The TMR^{rec} GRS was significantly higher in individuals with a cardiovascular event than those that did not have an event ($P=1.5 \times 10^{-2}$). Univariate Cox analysis showed that individuals in the top 20% of the GRS for TMR^{rec} were significantly more likely to have a cardiovascular event than those in the bottom 20% (HR [95% CI] of 1.07 [1.02–1.12]; $P=5.9 \times 10^{-3}$). No significant associations were found with the secondary end points for the 2 GRSs.

DISCUSSION

TMR is a recently developed ECG marker to measure the rate of variation of the T-wave morphology due to heart rate changes. TMR is associated with spatio-temporal heterogeneity of ventricular repolarization,¹¹ exposed in this cohort by exercise and recovery from exercise. The main findings of this study are (1) TMR^{rec} is significantly associated with cardiovascular events, all-cause mortality, and ventricular arrhythmias in a UK middle-aged population and (2) the identified loci for TMR^{rec} show a significant association with cardiovascular events despite limited heritability.

TMR^{rec} was an independent predictor of cardiovascular risk, after adjustment for conventional predictors (age, sex, diabetes mellitus, BMI, smoking, chronic kidney disease, and hypertension) and other ECG markers, including heart rate, corrected QT interval, and T-wave inversions in a general UK middle-aged population (Table 1). In this population, the majority of cardiovascular events were related to ischemic heart disease, and TMR^{rec} was associated with cardiovascular events in both ischemic and nonischemic individuals (Tables VA and VB in the [Data Supplement](#)). Well-established predictors of cardiovascular risk, like resting heart rate,²⁶ chronotropic incompetence, or heart rate recovery,²⁷ did not remain significantly associated with cardiovascular events after adjustment for ECG markers of ventricular repolarization (corrected QT interval, T-wave inversion, and TMR^{rec}). This suggests that ventricular repolarization abnormalities may play a more impor-

tant role in creating a substrate for malignant cardiovascular events than heart rate markers in a UK middle-aged population. The QRS duration was not associated with cardiovascular events in our population; this may be explained by our cohort being a low-risk population, and we had excluded individuals with previous cardiovascular events. We suggest that future analyses should incorporate additional ECG indices with similar proven findings in individuals undergoing an EST.²⁸

In our previous work, TMR predicted sudden cardiac death in a population of 651 chronic heart failure patients.^{4,5} In that work, TMR, derived from 24-hour ambulatory Holter recordings, was the strongest sudden cardiac death predictor compared with other markers, including left ventricular ejection fraction, QRS duration, or T-wave alternans.⁴ Interestingly, although the prevalence of ventricular arrhythmic events in the current study is too small to infer any robust conclusions (0.4% in UKB-EST, compared with 8.4% in the published chronic heart failure study), our results seem to support an association of TMR with sudden cardiac death (Table VII in the [Data Supplement](#)). In this study, TMR^{rec} was not significantly associated with atrial fibrillation.

We observed the heritability of TMR^{ex} and TMR^{rec} to be 3.5% and 4.9%, respectively, in our data set, suggesting that the mechanisms underlying TMR are largely affected by environmental factors. Despite low heritability, we identified 12 loci associated with TMR^{ex} and TMR^{rec} , 4 of which were common to both markers (Figure 4). Genetic variations at 4 of the 8 loci identified for TMR^{ex} have previously been associated with long-QT syndrome and QT in the general population: *KCNH2*, *KCNJ2*, *SCN5A*, and *KCNQ1*,²⁹ all proven regulators of cardiac excitation through regulation of the action potential duration and cardiac repolarizing channels.³⁰ *KCNQ1*, *KCNH2*, and *KCNJ2* underlie the major repolarising ventricular potassium currents, I_{Ks} , I_{Kr} , and I_{K1} , respectively. Variations in these currents might lead to changes in the T-wave morphology is entirely consistent with the known physiology. The signal involved in both TMR^{ex} and TMR^{rec} at the *KCNQ1* locus is particularly significant as the modulation of this current by rate and sympathetic tone is one of the main mechanisms of adaptation of repolarization.³¹ Candidate genes indicated at two of the TMR^{ex} loci were *PREP* and *SOX5* from Hi-C analyses, which have also been associated with heart rate response to exercise and to recovery.³²

For TMR^{rec} , 4 of the identified loci overlapped TMR^{ex} loci (*NOS1AP*, *SCN5A-SCN10A*, *KCNQ1*, and *SOX5*). Regarding the remaining 4 loci, the variant at *KLF12* has previously been reported to be associated with the QT interval, the ST-T segment, and QRS duration. Variants at the 3 remaining loci (*CAMKD2*, *SSBP3*, and *TSC22D2*) have not been associated with an ECG marker previously. Candidate genes at these loci

include: *SSBP3*, which encodes single-stranded DNA binding protein 3, and the TMR^{rec} variant identified at this locus has been reported to be associated with P-wave parameters, with its putative function being the transcriptional regulation of the alpha 2(1) collagen gene.³³ In addition, *TSC22D2* encodes a DNA binding transcription factor. Finally, the protein *CAMK2D* regulates calcium dynamics, which is central in cardiac physiology, as the key event leading to the excitation-contraction coupling and relaxation processes.³⁴

TMR was developed based on the hypothesis that it reflects changes in the dispersion of ventricular repolarization with heart rate.⁴ Although this is the first study that attempts to investigate the biological mechanisms underlying TMR, our predictive and genetic results indicate that TMR reflects relevant electrophysiological information. Our prediction results indicate TMR is providing prognostic information independent to resting QT (reflecting total duration of ventricular repolarization) or T-wave inversions (reflecting variations in the T-wave amplitude not captured by TMR). However, genetic analyses indicate there is a substantial overlap of loci with other ECG markers, thus shared biological processes. Future studies will investigate the relation between TMR and intracardiac indices of dispersion of repolarization, which is paramount to confirm its cardiovascular predictive utility.

Cardiovascular mortality remains the most common cause of death, with >4 million victims across Europe every year.¹ Over the past 2 decades, numerous prediction models have been developed,³⁵ including the Framingham³⁶ and SCORE³⁷ models. This prediction can be further improved by including additional validated risk markers into the models. Table XVI in the [Data Supplement](#) shows the reclassification results for the addition of TMR^{rec} ≥ 0.115 to the SCORE model (Methods in the [Data Supplement](#)), indicating that TMR adds information on risk prediction beyond traditional risk factors. In addition, the significant association between the GRS for TMR^{rec} and cardiovascular events in the FULL-UKB cohort supports its potential as a cardiovascular risk predictor in high-risk populations, albeit with small HRs possibly due to the low number of events. Future work should combine ECG and genetic markers into one score (ECG markers could only be derived from EST-UKB in this study), which may show complementary cardiovascular predictive value of both TMR^{rec} and its GRS.

CONCLUSIONS

We have conducted a systematic investigation of the genetic basis of ventricular repolarization and its influence in modulating cardiovascular risk through the analysis of the T-wave morphology. We demonstrate that TMR and the GRS for TMR^{rec} are significantly associated with cardiovascular risk in a UK middle-aged population

and that TMR reflects relevant biological mechanisms influencing the risk of cardiovascular events.

ARTICLE INFORMATION

Received February 12, 2019; accepted August 20, 2019.

The Data Supplement is available at <https://www.ahajournals.org/doi/suppl/10.1161/CIRCEP.119.007549>.

Correspondence

Julia Ramirez, PhD, Clinical Pharmacology, William Harvey Research Institute, Barts and The London School of Medicine and Dentistry, Queen Mary University of London, London EC1M 6BQ, United Kingdom, Email j.ramirez@qmul.ac.uk or Patricia B. Munroe, PhD, Clinical Pharmacology, William Harvey Research Institute, Barts and The London School of Medicine and Dentistry, Queen Mary University of London, London EC1M 6BQ, United Kingdom, Email p.b.munroe@qmul.ac.uk

Affiliations

Clinical Pharmacology, William Harvey Research Institute, Barts and The London School of Medicine and Dentistry (J.R., S.v.D., A.T., M.O., P.B.M.), Centre for Advanced Cardiovascular Imaging, William Harvey Research Institute (N.A.), and National Institute of Health Research Barts Cardiovascular Biomedical Research Centre, Barts and The London School of Medicine and Dentistry (A.T., P.B.M.), Queen Mary University of London, United Kingdom. Institute of Cardiovascular Science, University College London, United Kingdom (J.R., S.v.D., P.D.L., M.O.). Barts Heart Centre, St Bartholomew's Hospital, London, United Kingdom (N.A., P.D.L.). Biomedical Signal Interpretation and Computational Simulation (BSI-CoS) group, Aragón Institute of Engineering Research, IIS Aragón, University of Zaragoza, Spain (P.L., E.P.). Biomedical Research Networking Center in Bioengineering, Biomaterials and Nanomedicine (CIBER-BBN), Spain (P.L., E.P.).

Acknowledgments

We would like to acknowledge the contribution of Alejandro Bona with the design of the graphical abstract.

Sources of Funding

This research has been conducted using the UKB Resource (application 8256) and is supported by grant MR/N025083/1 from the Medical Research Council (MRC), by the National Institutes of Health Research (NIHR) Cardiovascular Biomedical Centre at Barts and The London, Queen Mary University of London (QMUL), by the People Programme of the European Union's Seventh Framework Programme grant n° 608765 and Marie Skłodowska-Curie grant n° 786833, by the University College London Hospital Biomedicine NIHR, Barts Heart Centre Biomedical Research Centre, by grant ERC-2014-StG 638284 from the European Research Council (ERC), by project DPI2016-75458-R and by Reference Group BSICoS T39-17R cofunded by Fondo Europeo de Desarrollo Regional 2014–2020. This research utilized Queen Mary's Apocrita High-performance cluster facility, supported by QMUL Research-IT. <http://doi.org/10.5281/zenodo.438045>.

Disclosures

None.

REFERENCES

1. Townsend N, Wilson L, Bhatnagar P, Wickramasinghe K, Rayner M, Nichols M. Cardiovascular disease in Europe: epidemiological update 2016. *Eur Heart J*. 2016;37:3232–3245. doi: 10.1093/eurheartj/ehw334
2. Pak HN, Hong SJ, Hwang GS, Lee HS, Park SW, Ahn JC, Moo Ro Y, Kim YH. Spatial dispersion of action potential duration restitution kinetics is associated with induction of ventricular tachycardia/fibrillation in humans. *J Cardiovasc Electrophysiol*. 2004;15:1357–1363. doi: 10.1046/j.1540-8167.2004.03569.x
3. Nash MP, Bradley CP, Sutton PM, Clayton RH, Kallis P, Hayward MP, Paterson DJ, Taggart P. Whole heart action potential duration resti-

- tution properties in cardiac patients: a combined clinical and modeling study. *Exp Physiol*. 2006;91:339–354. doi: 10.1113/expphysiol.2005.031070
4. Ramírez J, Orini M, Mincholé A, Monasterio V, Cygankiewicz I, Luna ABd, Martínez JP, Pueyo E, Laguna P. T-wave morphology restitution predicts sudden cardiac death in patients with chronic heart failure. *J Am Heart Assoc*. 2017;6:e005310. doi:10.1161/JAHA.116.005310
 5. Ramírez J, Orini M, Mincholé A, Monasterio V, Cygankiewicz I, Bayés de Luna A, Martínez JP, Laguna P, Pueyo E. Sudden cardiac death and pump failure death prediction in chronic heart failure by combining ECG and clinical markers in an integrated risk model. *PLoS One*. 2017;12:e0186152. doi: 10.1371/journal.pone.0186152
 6. Hodkinson EC, Neijts M, Sadrieh A, Imtiaz MS, Baumert M, Subbiah RN, Hayward CS, Boomsma D, Willemsen G, Vandenberg JJ, Hill AP, De Geus E. Heritability of ECG biomarkers in the Netherlands twin registry measured from Holter ECGs. *Front Physiol*. 2016;7:154. doi: 10.3389/fphys.2016.00154
 7. Hajek C, Guo X, Yao J, Hai Y, Johnson WC, Frazier-Wood AC, Post WS, Psaty BM, Taylor KD, Rotter JL. Coronary heart disease genetic risk score predicts cardiovascular disease risk in men, not women. *Circ Genom Precis Med*. 2018;11:e002324. doi: 10.1161/CIRCGEN.118.002324
 8. Sudlow C, Gallacher J, Allen N, Beral V, Burton P, Danesh J, Downey P, Elliott P, Green J, Landray M, Liu B, Matthews P, Ong G, Pell J, Silman A, Young A, Sprosen T, Peakman T, Collins R. UK Biobank: an open access resource for identifying the causes of a wide range of complex diseases of middle and old age. *PLoS Med*. 2015;12:e1001779. doi: 10.1371/journal.pmed.1001779
 9. Orini M, Pueyo E, Laguna P, Bailon R. A time-varying nonparametric methodology for assessing changes in QT variability unrelated to heart rate variability. *IEEE Trans Biomed Eng*. 2018;65:1443–1451. doi: 10.1109/TBME.2017.2758925
 10. Srinivasan NT, Orini M, Providencia R, Simon R, Lowe M, Segal OR, Chow AW, Schilling RJ, Hunter RJ, Taggart P, Lambiase PD. Differences in the upslope of the precordial body surface ECG T wave reflect right to left dispersion of repolarization in the intact human heart. *Heart Rhythm*. 2019;16:943–951. doi: 10.1016/j.hrthm.2018.12.006
 11. Ramírez J, Orini M, Tucker JD, Pueyo E, Laguna P. Variability of ventricular repolarization dispersion quantified by time-warping the morphology of the T-Waves. *IEEE Trans Biomed Eng*. 2017;64:1619–1630. doi: 10.1109/TBME.2016.2614899
 12. Bazett HC. An analysis of the time-relations of electrocardiograms. *Ann Noninvasive Electrocardiol*. 1997;2:177–194.
 13. Malhotra A, Dhutia H, Gati S, Yeo TJ, Dores H, Bastiaenen R, Narain R, Merghani A, Finocchiaro G, Sheikh N, Steriotis A, Zaidi A, Millar L, Behr E, Tome M, Papadakis M, Sharma S. Anterior T-wave inversion in young white athletes and nonathletes: prevalence and significance. *J Am Coll Cardiol*. 2017;69:1–9. doi: 10.1016/j.jacc.2016.10.044
 14. Robin X, Turck N, Hainard A, Tiberti N, Lisacek F, Sanchez JC, Müller M. pROC: an open-source package for R and S+ to analyze and compare ROC curves. *BMC Bioinformatics*. 2011;12:77. doi: 10.1186/1471-2105-12-77
 15. Loh PR, Bhatia G, Gusev A, Finucane HK, Bulik-Sullivan BK, Pollack SJ, de Candia TR, Lee SH, Wray NR, Kendler KS, O'Donovan MC, Neale BM, Patterson N, Price AL; Schizophrenia Working Group of Psychiatric Genomics Consortium. Contrasting genetic architectures of schizophrenia and other complex diseases using fast variance-components analysis. *Nat Genet*. 2015;47:1385–1392. doi: 10.1038/ng.3431
 16. Loh PR, Tucker G, Bulik-Sullivan BK, Vilhjálmsson BJ, Finucane HK, Salem RM, Chasman DI, Ridker PM, Neale BM, Berger B, Patterson N, Price AL. Efficient bayesian mixed-model analysis increases association power in large cohorts. *Nat Genet*. 2015;47:284–290. doi: 10.1038/ng.3190
 17. Turley P, Walters RK, Maghziyan O, Okbay A, Lee JJ, Fontana MA, Nguyen-Viet TA, Wedow R, Zacher M, Furlotte NA, Magnusson P, Oskarsson S, Johannesson M, Visscher PM, Laibson D, Cesarini D, Neale BM, Benjamin DJ; 23andMe Research Team; Social Science Genetic Association Consortium. Multi-trait analysis of genome-wide association summary statistics using MTAG. *Nat Genet*. 2018;50:229–237. doi: 10.1038/s41588-017-0009-4
 18. Yang J, Lee SH, Goddard ME, Visscher PM. GCTA: a tool for genome-wide complex trait analysis. *Am J Hum Genet*. 2011;88:76–82. doi: 10.1016/j.ajhg.2010.11.011
 19. McLaren W, Gil L, Hunt SE, Riat HS, Ritchie GR, Thormann A, Flicek P, Cunningham F. The ensemble variant effect predictor. *Genome Biol*. 2016;17:122. doi: 10.1186/s13059-016-0974-4
 20. Schmitt AD, Hu M, Jung I, Xu Z, Qiu Y, Tan CL, Li Y, Lin S, Lin Y, Barr CL, Ren B. A compendium of chromatin contact maps reveals spatially active regions in the human genome. *Cell Rep*. 2016;17:2042–2059. doi: 10.1016/j.celrep.2016.10.061
 21. Staley JR, Blackshaw J, Kamat MA, Ellis S, Surendran P, Sun BB, Paul DS, Freitag D, Burgess S, Danesh J, Young R, Butterworth AS. PhenoScanner: a database of human genotype-phenotype associations. *Bioinformatics*. 2016;32:3207–3209. doi: 10.1093/bioinformatics/btw373
 22. Raudvere U, Kolberg L, Kuzmin I, Arak T, Adler P, Peterson H, Vilo J. g:Profiler: a web server for functional enrichment analysis and conversions of gene lists (2019 update). *Nucleic Acids Res*. 2019;47(W1):W191–W198. doi: 10.1093/nar/gkz369
 23. Nielsen JB, Thorolfsdottir RB, Fritsche LG, Zhou W, Skov MW, Graham SE, Herron TJ, McCarthy S, Schmidt EM, Sveinbjornsson G, Surakka I, Mathis MR, Yamazaki M, Crawford RD, Gabrielsen ME, Skogholt AH, Holmen OL, Lin M, Wolford BN, Dey R, Dalen H, Sulem P, Chung JH, Backman JD, Arnar DO, Thorsteinsdottir U, Baras A, O'Dushlaine C, Holst AG, Wen X, Hornsby W, Dewey FE, Boehnke M, Khetarpal S, Mukherjee B, Lee S, Kang HM, Holm H, Kitzman J, Shavit JA, Jalife J, Brummett CM, Teslovich TM, Carey DJ, Gudbjartsson DF, Stefansson K, Abecasis GR, Hveem K, Willer CJ. Biobank-driven genomic discovery yields new insight into atrial fibrillation biology. *Nat Genet*. 2018;50:1234–1239. doi: 10.1038/s41588-018-0171-3
 24. Bulik-Sullivan BK, Loh PR, Finucane HK, Ripke S, Yang J, Patterson N, Daly MJ, Price AL, Neale BM; Schizophrenia Working Group of the Psychiatric Genomics Consortium. LD Score regression distinguishes confounding from polygenicity in genome-wide association studies. *Nat Genet*. 2015;47:291–295. doi: 10.1038/ng.3211
 25. Lewis CM, Euesden J, O'Reilly PF. PRSice: polygenic risk score software. *Bioinformatics*. 2014;31:1466–1468. doi:10.1093/bioinformatics/btu848
 26. Kannel WB, Kannel C, Paffenbarger RS Jr, Cupples LA. Heart rate and cardiovascular mortality: the Framingham Study. *Am Heart J*. 1987;113:1489–1494. doi: 10.1016/0002-8703(87)90666-1
 27. Morshedi-Meibodi A, Larson MG, Levy D, O'Donnell CJ, Vasan RS. Heart rate recovery after treadmill exercise testing and risk of cardiovascular disease events (The Framingham Heart Study). *Am J Cardiol*. 2002;90:848–852. doi: 10.1016/s0002-9149(02)02706-6
 28. Kenttä T, Viik J, Karsikas M, Seppänen T, Nieminen T, Lehtimäki T, Nikus K, Lehtinen R, Kähönen M, Huikuri HV. Postexercise recovery of the spatial QRS/T angle as a predictor of sudden cardiac death. *Heart Rhythm*. 2012;9:1083–1089. doi: 10.1016/j.hrthm.2012.02.030
 29. Goldenberg I, Moss AJ. Long QT syndrome. *J Am Coll Cardiol*. 2008;51:2291–2300. doi: 10.1016/j.jacc.2008.02.068
 30. Roder K, Werdich AA, Li W, Liu M, Kim TY, Organ-Darling LE, Moshal KS, Hwang JM, Lu Y, Choi BR, MacRae CA, Koren G. RING finger protein RNF207, a novel regulator of cardiac excitation. *J Biol Chem*. 2014;289:33730–33740. doi: 10.1074/jbc.M114.592295
 31. Finlay M, Harmer SC, Tinker A. The control of cardiac ventricular excitability by autonomic pathways. *Pharmacol Ther*. 2017;174:97–111. doi: 10.1016/j.pharmthera.2017.02.023
 32. Ramírez J, Duijvenboden SV, Ntalla I, Mifsud B, Warren HR, Tzani E, Orini M, Tinker A, Lambiase PD, Munroe PB. Thirty loci identified for heart rate response to exercise and recovery implicate autonomic nervous system. *Nat Commun*. 2018;9:1947. doi: 10.1038/s41467-018-04148-1
 33. Bayarsaihan D, Soto RJ, Lukens LN. Cloning and characterization of a novel sequence-specific single-stranded-DNA-binding protein. *Biochem J*. 1998;331(pt 2):447–452. doi: 10.1042/bj3310447
 34. Mattiazzi A, Bassani RA, Escobar AL, Palomeque J, Valverde CA, Vila Petroff M, Bers DM. Chasing cardiac physiology and pathology down the CaMKII cascade. *Am J Physiol Heart Circ Physiol*. 2015;308:H1177–H1191. doi: 10.1152/ajpheart.00007.2015
 35. Damen JA, Hooft L, Schuit E, Debray TP, Collins GS, Tzoulaki I, Lassale CM, Siontis GC, Chiochia V, Roberts C, Schlüssel MM, Gerry S, Black JA, Heus P, van der Schouw YT, Peelen LM, Moons KG. Prediction models for cardiovascular disease risk in the general population: systematic review. *BMJ*. 2016;353:i2416. doi: 10.1136/bmj.i2416
 36. Anderson KM, Odell PM, Wilson PW, Kannel WB. Cardiovascular disease risk profiles. *Am Heart J*. 1991;121(1 pt 2):293–298. doi: 10.1016/0002-8703(91)90861-b
 37. Conroy RM, Pyörälä K, Fitzgerald AP, Sans S, Menotti A, De Backer G, De Bacquer D, Ducimetière P, Jousilahti P, Keil U, Njølstad I, Oganov RG, Thomsen T, Tunstall-Pedoe H, Tverdal A, Wedel H, Whincup P, Wilhelmsen L, Graham IM; SCORE project group. Estimation of ten-year risk of fatal cardiovascular disease in Europe: the SCORE project. *Eur Heart J*. 2003;24:987–1003. doi: 10.1016/s0195-668x(03)00114-3

SUPPLEMENTAL MATERIAL

Supplemental Methods

Study population

The exercise protocol was adapted according to participants' risk factors. Participants were only included in the study if they were allowed to cycle at 50% or 30% of their maximum workload (no risk to minimum risk). If the heart rate reached the pre-set maximum heart rate level (75% of age-predicted maximum heart rate), the test was stopped. Also, if the participant reported chest pain, felt faint, dizzy or unwell, the test was also stopped (<https://biobank.ctsu.ox.ac.uk/crystal/docs/Cardio.pdf>). We only included participants who terminated the exercise stress test with any discomfort and with a heart rate lower than the pre-set maximum heart rate level.

Exclusions

Individuals were excluded based on existing medical conditions known to affect heart rate (atrial fibrillation, history of myocardial infarction or heart failure, (supra)-ventricular tachycardia, atrioventricular nodal re-entrant tachycardia, second or third degree atrioventricular block, bundle branch block and use of a pacemaker), individuals with a previous CV event (matching the codes from Supplemental Table 1) and/or individuals on heart rate altering medications (non-dihydropyridine calcium antagonists (Anatomic Therapeutic Chemical (ATC) code C08D, digoxin (ATC code C01AA5), and amiodarone (ATC code C01BD01)). Individuals with an RR interval (inverse of heart rate) change between resting and peak exercise, or between peak exercise and recovery, less than 10 ms or poor quality ECG recording were also excluded.

End points

The cause of death was defined according to the *ICD-10* codes. Date of death was obtained from death certificates held by the National Health Service (NHS) Information Centre

and the NHS Central Register Scotland for participants from England and Wales and participants from Scotland, respectively. CV diagnoses were captured using the “Spell and Episode” category from the Hospital Episode Statistics records. This category contains main and secondary diagnoses, coded according to *ICD-10*, made during the hospital inpatient stay. The main diagnoses are those taken to be the main reason for hospital admission, while secondary diagnoses are more often contributory or underlying conditions. We used both the main and secondary diagnoses for recording prevalent and incident risk factors, conditions and events. Date of the event was defined as the date of the first diagnosis.

ECG lead placement during the exercise test

The cardio assessment involved a 1 lead (lead I) ECG recording (AM-USB 6.5, Cardiosoft v6.51) at a frequency of 500 Hz. The ECG was recorded using four electrodes placed on the right and left antecubital fossa and wrist (Figure R1) and stored in an xml-file of Cardiosoft (<https://biobank.ctsu.ox.ac.uk/crystal/docs/Cardio.pdf>).

Pre-processing of the ECG signals

Pre-processing of the ECG signals from the EST-UKB cohort included low-pass filtering at 50 Hz to remove electric and muscle noise but still allow QRS detection¹. Baseline wander was removed by further high-pass filtering the ECG signals at 0.5 Hz.

Computation of other ECG markers

For the derivation of QTc, we first detected the heartbeats using a fully automated in-house developed delineation system^{1,2}. Then, we computed the averaged ECG waveform by collecting all heartbeats in a 15-s window at resting stage. Finally, the QT interval was measured as the interval between the QRS-onset and the T-wave end from the averaged ECG waveform at rest. We, then, corrected the QT interval using Bazett’s formula³.

The TWI marker reflects if the polarity of the T-wave changes between resting and peak exercise stages (i.e. goes from positive to inverted, or from inverted to positive). A

positive T-wave was determined if the amplitude of the T-wave peak was larger than the average amplitude values at T-wave onset and T-wave offset. An inverted T-wave was determined if the amplitude of the T-wave peak was more negative than the average amplitude values at T-wave onset and T-wave offset.

Statistical analyses

Based on previous papers reporting that the log-rank statistic optimization criteria is more robust than the AUC criteria for imbalanced datasets^{4,5}, we derived the cut-off values for TMR^{ex} and TMR^{rec} in the training set using this method. The criteria was defined as the one that simultaneously verified the following criteria: (i) it was associated with a P -value $< 10^{-3}$ (Supplemental Figures 4 and 5, panel A) (ii) it corresponded to a local maximum of the hazard ratio function from univariate Cox models (Supplemental Figures 4 and 5, panel B), and (iii) the proportion of individuals in the high-risk and low-risk groups was $> 10\%$ and $> 50\%$, respectively (Supplemental Figures 4 and 5, panels C and D). If more than one cut-off value met these criteria, the one associated with the highest hazard ratio was used. The predictive value of the optimal cut-off values was then tested in the test group.

The net reclassification improvement (NRI)⁶ was used to quantify the added predictive value of $TMR^{rec} \geq 0.115$ beyond that from the model including all traditional risk factors for CV risk in the multivariate Cox analysis (age, sex, HTN, cholesterol and smoking status). We derived the NRI in the test set and we followed the same criteria as in our survival analyses, we predicted risk at 7 years (2,520 days) and individuals who died from causes not included in the primary endpoint were censored at the time of death. Bootstrapping (100 iterations) was performed to derive confidence intervals. The CV risk categories used for the NRI analysis were 1%, 1 to 5%, 5 to 10% and $\geq 10\%$ ⁷. A version of NRI appropriate for survival analyses was computed using the Kaplan–Meier method⁶. NRI was computed using the package “nricens” in R.

Genetic analyses

Individuals with poor genotype quality (high missingness or heterozygosity or discordance between the self-reported sex and the sex inferred from the genotypes) were excluded from the EST-UKB cohort and the FULL-UKB cohort (see later) ⁸. All genetic analyses were restricted to individuals of European ancestry (Figure 1 and Supplementary Figure 2).

First, we selected model SNVs from the genotyped SNVs using PLINK 1.9⁹. This selection was based on previously published criteria¹⁰. Then, we estimated the proportion of TMR^{ex} and TMR^{rec} explained by additive genetic variation (heritability) using a variance components method (BOLT-REML)¹¹, with the model SNVs and ~ 9 million imputed variants with MAF \geq 1% and imputation quality (INFO) $>$ 0.3.

Next, we randomly divided the EST-UKB dataset into discovery ($N = 29,393$) and replication ($N = 22,382$) datasets. To ensure that there was no overlap with the discovery samples, we removed a total of $N = 532$ first- and second-degree related individuals (kinship coefficient $>$ 0.88) from the replication cohort as indicated from UK Biobank⁸. Then, we performed a GWAS for TMR^{ex} and TMR^{rec} in the discovery dataset using a linear mixed model method (BOLT-LMM)¹² under the additive genetic model, including ~9 million imputed SNVs with MAF \geq 1% and INFO $>$ 0.3 from the latest release from UKB. For TMR^{ex} we included the following covariates: sex, age, body mass index (BMI), resting RR, RR difference between peak exercise and resting (ΔRR^{ex}) and a binary indicator variable for the genotyping array (UK Biobank versus UK BiLEVE). For TMR^{rec} , we included sex, age, BMI, recovery RR, RR difference between peak exercise and recovery (ΔRR^{rec}) and the genetic array.

A GWAS for both markers was also performed in the replication dataset. All SNVs with $P < 1 \times 10^{-6}$ from the discovery analysis for both markers were compiled and SNVs were mapped to individual loci based on a genomic distance of $>$ 500 Kb to each side of another SNV and based on linkage disequilibrium (LD). If multiple SNVs fitted the selection criteria for a single region, only the SNV with the smallest P value was considered for follow up. We

reviewed each selected SNV to check for unrealistically high effect sizes, large standard errors, and none was observed. Locus Zoom plots were produced for all selected SNVs and these were carefully reviewed. Six variants for TMR^{ex} and seven variants for TMR^{rec} were taken forward into replication. Replication was confirmed if P (one-tailed) $\leq 0.05/6 = 8.3 \times 10^{-3}$ for TMR^{ex} and P (one-tailed) $\leq 0.05/7 = 7.1 \times 10^{-3}$ for TMR^{rec} and the effect was in the direction observed in discovery analyses for each marker in the replication cohort.

Finally, we performed a full dataset GWAS for each marker using BOLT-LMM in EST-UKB¹². Additional loci for each marker reaching a genome-wide significance threshold ($P \leq 5 \times 10^{-8}$) were reported.

Multi-Trait Analysis of GWAS (MTAG)¹³ enables the joint analysis of summary statistics from GWASs of correlated markers to boost the statistical power of each single-marker GWAS. We applied MTAG to the summary statistics for TMR^{ex} and TMR^{rec} , since the markers were correlated ($\rho=0.56$) to leverage additional loci discovery for each marker, loci with $P \leq 5 \times 10^{-8}$ were reported.

A secondary signal would be declared if: (i) the newly identified SNV original P value was lower than 1×10^{-6} ; (ii) there was less than a 1.5-fold difference between the lead SNV and secondary association P values on a $-\log_{10}$ scale, i.e., if $-\log_{10}(P_{lead}) / -\log_{10}(P_{sec}) < 1.5$; and (iii) if there was less than a 1.5-fold difference between the main association and conditional association P values on a $-\log_{10}$ scale, i.e., if $-\log_{10}(P_{sec}) / -\log_{10}(P_{cond}) < 1.5$.

The per cent variance explained of each marker was calculated by estimating the residuals from the regression model against the covariates used in each respective genetic model. We then fitted a second linear model for the marker residuals with all the identified variants plus the top ten principal components. The per cent variance explained was the difference between the adjusted R-squared parameters from each model.

Bioinformatic analyses

To explore shared mechanisms of disease, we assessed association of our identified SNVs (and their proxies, $r^2 \geq 0.8$) with other traits from published GWAS using PhenoScanner¹⁴. Using the University of California, Santa Cruz (UCSC) website, we annotated each TMR lead SNV to provide nearest genes and those located within 5kb. At the variant level, we used Variant Effect Predictor¹⁵ to obtain comprehensive functional characterization of variants, including their gene location, conservation, and amino acid substitution impact based on a range of prediction tools including SIFT and PolyPhen-2.

We evaluated all SNVs in LD ($r^2 \geq 0.8$) with our validated lead SNVs for evidence of mediation of expression quantitative trait loci (eQTLs) using the GTEx database, focusing on loci with the strongest evidence of eQTL associations in brain, heart and adrenal tissue. In addition, genetic variants may have a causal effect through regulatory chromatin interactions. We investigated variants at the 12 independent loci associated with *TMR^{ex}* and *TMR^{rec}*. We identified variants with regulatory potential using RegulomeDB¹⁶ and found genes whose promoter regions form significant chromatin interaction with them from a range of tissues, we report results from brain, heart and adrenal Hi-C data. We found the most significant promoter interactions for all potential regulatory SNVs (RegulomeDB score ≤ 5) in LD ($r^2 \geq 0.8$) with our sentinel SNVs and chose the interactors with the SNVs of highest regulatory potential to annotate the loci.

Subsequently, we performed pathway analyses using g:profiler¹⁷ including our candidate genes. The National Center for Biotechnology Information (NCBI) Gene database and GeneCards®: The Human Gene Database were used to obtain official full names and, where relevant, common aliases for each candidate gene product. NCBI's PubMed was used to interrogate primary literature pertaining to gene function. We also reviewed gene-specific animal models using International Mouse Phenotyping Consortium¹⁸ and the Mouse Genome Informatics database¹⁹. Finally, to investigate pleiotropy of our candidate genes, we queried them at the GWAS catalogue²⁰ and at the UKBiobank ICD PheWeb for case-control phenotypes.

Genetic risk score analyses

Variants with minor allele frequency < 0.05 and imputation quality ≤ 0.3 were removed from the calculation. PRSice clumped variants to obtain SNVs in linkage equilibrium ($r^2 < 0.1$) within a 250 kb window. Multiple GRSs were computed at a large number of GWAS P -value thresholds ranging from 1×10^{-4} to 0.5 with 5×10^{-5} increments. PRSice then performed a logistic regression analysis between each GRS and the primary endpoint, adjusting for age, sex, diabetes, cholesterol, BMI, systolic blood pressure (SBP), the genotyping array and the 10 first genetic principal components. The optimal GRS was then chosen as the one with the smallest P -value.

Supplemental Tables

**Supplemental Table 1: ICD-10 codes used in follow-up analyses
Cardiovascular events**

Code	Definition
I21	Acute myocardial infarction
I210	Acute transmural myocardial infarction of anterior wall
I211	Acute transmural myocardial infarction of inferior wall
I212	Acute transmural myocardial infarction of other sites
I213	Acute transmural myocardial infarction of unspecified site
I214	Acute subendocardial myocardial infarction
I219	Acute myocardial infarction, unspecified
I22	Subsequent myocardial infarction
I220	Subsequent myocardial infarction of anterior wall
I221	Subsequent myocardial infarction of inferior wall
I228	Subsequent myocardial infarction of other sites
I229	Subsequent myocardial infarction of unspecified site
I24	Other acute ischaemic heart diseases
I248	Other forms of acute ischaemic heart disease
I249	Acute ischaemic heart disease, unspecified
I25	Chronic ischaemic heart disease
I250	Atherosclerotic cardiovascular disease, so described
I251	Atherosclerotic heart disease
I253	Aneurysm of heart
I254	Coronary artery aneurysm
I255	Ischaemic cardiomyopathy
I256	Silent myocardial ischaemia
I258	Other forms of chronic ischaemic heart disease
I259	Chronic ischaemic heart disease, unspecified
I46	Cardiac arrest
I460	Cardiac arrest with successful resuscitation
I461	Sudden cardiac death, so described
I469	Cardiac arrest, unspecified
I470	Reentry ventricular arrhythmia
I472	Ventricular tachycardia
I490	Ventricular fibrillation and flutter
I499	Cardiac arrhythmia, unspecified
I50	Heart failure
I500	Congestive heart failure
I501	Left ventricular failure
I509	Heart failure, unspecified
I64	Stroke, not specified as haemorrhage or infarction

Ventricular arrhythmic events

Code	Definition
-------------	-------------------

I460	Cardiac arrest with successful resuscitation
I461	Sudden cardiac death, so described
I469	Cardiac arrest, unspecified
I472	Ventricular tachycardia
I490	Ventricular fibrillation and flutter
I499	Cardiac arrhythmia, unspecified

Atrial fibrillation

I480	Paroxysmal atrial fibrillation
I481	Persistent atrial fibrillation
I482	Chronic atrial fibrillation
I489	Atrial fibrillation and atrial flutter, unspecified
I48	Atrial fibrillation and flutter

Supplemental Table 2: Patient characteristics in the EST-UKB and FULL-UKB cohorts

	EST-UKB cohort	FULL-UKB cohort
Study characteristics		
Number of subjects, N	55,222	360,631
Median follow-up (IQR), months	84 (3.3)	101.1 (15.1)
Cardiovascular events, n(%)	1,743 (3.2)	18,997 (5.3)
All-cause mortality events, n(%)	979 (1.8)	12,081 (3.3)
Arrhythmic events, n(%)	198 (0.4)	2,040 (0.6)
Atrial fibrillation events, n(%)	1,112 (2.0)	14,517 (4.0)
Patients characteristics		
Median age (IQR), years	58 (13)	58 (13)
Females, n(%)	29,553 (53.5)	199,838 (55.4)
Diabetes mellitus, n(%)	2,305 (4.2)	15,857 (4.4)
Median BMI (IQR), kg/m ²	26.4 (5.4)	26.7 (5.7)
Hypertensive Stage 1	11,978 (21.7)	70,940 (19.7)
Hypertensive Stage 2	11,978 (43.3)	156,987 (43.5)
Previous or current smoker, n(%)	23,403 (42.4)	163,450 (45.3)
CKD, n(%)	44 (0.1)	467 (0.1)
High cholesterol, n(%)	6,297 (11.4)	40,431 (11.2)

*IQR, interquartile range; BMI, body mass index; CKD, chronic kidney disease

Hypertensive Stage 1 defined as $130 \text{ mmHg} \leq \text{SBP} < 140 \text{ mmHg}$ or $85 \text{ mmHg} \leq \text{DBP} < 90 \text{ mmHg}$

Hypertensive Stage 2 defined as $\text{SBP} \geq 140 \text{ mmHg}$ or $\text{DBP} \geq 90 \text{ mmHg}$

Supplemental Table 3: Characteristics of the study population in the cardiovascular events and in the cardiovascular event-free groups

Characteristics	Cardiovascular events group	Cardiovascular event-free group	P-value
	N = 1,743	N = 53,479	
Median age (IQR), years	62 (9)	58 (13)	2.20E-16
Males, n(%)	1,243 (71.3)	24,426 (45.7)	2.20E-16
Diabetes mellitus, n(%)	178 (10.2)	2,127 (4.0)	2.20E-16
Median BMI (IQR), kg/m ²	27.8 (5.6)	26.4 (5.3)	2.20E-16
Hypertensive Stage 1	364 (20.9)	11,614 (21.7)	2.20E-16
Hypertensive Stage 2	1,029 (59.0)	22892 (42.8)	2.20E-16
Previous or current smoker, n(%)	890 (51.1)	22,513 (42.1)	1.20E-13
CKD, n(%)	4 (0.2)	40 (0.1)	5.00E-02
High cholesterol, n(%)	336 (19.3)	5,961 (11.1)	2.20E-16
Median resting heart rate (IQR), bpm	71.3 (16.6)	70.3 (15.0)	2.60E-04
Median heart rate response to exercise (IQR), bpm	36.8 (15.4)	40.8 (16.5)	2.20E-16
Median heart rate response to recovery (IQR), bpm	23.7 (12.0)	27.5 (13.0)	2.20E-16
Median QTc (IQR), ms ⁻¹	399.5 (33.4)	395.6 (30.4)	4.70E-09
Median QRS duration (IQR), ms	68 (17.3)	68 (18)	5.10E-01
T-wave inversions, n(%)	8 (0.5)	84 (0.2)	8.50E-03
Median TMR during exercise (IQR), d.u.	0.046 (0.034)	0.043 (0.029)	2.60E-08
Median TMR during recovery (IQR), d.u.	0.053 (0.060)	0.044 (0.044)	2.20E-16

*IQR, interquartile range; BMI, body mass index; CKD, chronic kidney disease; bpm, beats per minute; QTC, corrected QT interval; TMR, T-wave morphology restitution; d.u., dimensionless units

Hypertensive Stage 1 defined as 130 mmHg ≤ SBP < 140 mmHg or 85 mmHg ≤ DBP < 90 mmHg

Hypertensive Stage 2 defined as SBP ≥ 140 mmHg or DBP ≥ 90 mmHg

Supplemental Table 4: Spearman correlation coefficient between TMR during exercise and recovery and covariates

	TMR during exercise	TMR during recovery	Age	Sex	diabetes	high cholesterol	HTN	Smoker	CKD	BMI	Resting heart rate	QTc	QRS duration	T-wave inversion	Heart rate response to exercise	Heart rate response to recovery
TMR during exercise	1.000	0.484	0.061	0.066	0.066	0.040	0.049	0.010	0.007	0.008	0.438	0.028	0.051	0.053	-0.219	-0.188
TMR during recovery	0.484	1.000	0.011	0.014	0.013	0.074	0.079	0.031	0.020	0.044	0.367	0.055	0.033	0.050	-0.117	-0.388

*BMI, body mass index; HTN, hypertension; CKD, chronic kidney disease; QTc, corrected QT interval; TMR, T-wave morphology restitution; d.u., dimensionless units

Supplemental Table 5A: Association with ischemic events

	Univariate		Multivariate	
	HR (95% CI)	p	HR (95% CI)	p
Clinical Variables				
Age [per 1 SD]	1.84 (1.72-1.96)	<2x10⁻¹⁶	1.65 (1.55-1.77)	<2x10⁻¹⁶
Sex (male)	3.32 (2.94-3.75)	<2x10⁻¹⁶	2.98 (2.62-3.38)	<2x10⁻¹⁶
Diabetes (yes)	2.87 (2.41-3.41)	<2x10⁻¹⁶	1.61 (1.34-1.93)	3.20E-07
High cholesterol (yes)	2.15 (1.89-2.46)	<2x10⁻¹⁶	1.23 (1.07-1.41)	3.70E-03
BMI [per 1 SD]	1.29 (1.23-1.35)	<2x10⁻¹⁶	1.18 (1.12-1.25)	5.10E-09
Hypertensive Stage 1	1.72 (1.45-2.04)	5.00E-10	1.19 (1.00-1.42)	4.70E-02
Hypertensive Stage 2	2.49 (2.17-2.87)	<2x10⁻¹⁶	1.36 (1.17-1.58)	4.30E-05
Previous or current smoker (yes)	1.43 (1.28-1.59)	1.00E-10	1.12 (1.00-1.25)	4.70E-02
ECG variables				
Resting heart rate [per 1 SD]	1.07 (1.01-1.13)	1.60E-02	0.96 (0.90-1.03)	2.80E-01
Heart rate response to exercise [per 1 SD]	0.71 (0.67-0.76)	<2x10⁻¹⁶	1.02 (0.93-1.11)	6.90E-01
Heart rate response to recovery [per 1 SD]	0.74 (0.71-0.78)	<2x10⁻¹⁶	0.98 (0.91-1.05)	5.60E-01
Corrected QT [per 1 SD]	1.11 (1.06-1.17)	4.70E-05	1.08 (1.02-1.14)	1.10E-02
T-wave inversion (yes)	3.41 (1.70-6.83)	5.40E-04	2.95 (1.46-5.94)	2.60E-03
TMR during exercise [per 1 SD]	1.14 (1.09-1.20)	5.70E-09	1.03 (0.97-1.09)	3.00E-01
TMR during recovery [per 1 SD]	1.21 (1.16-1.26)	<2x10⁻¹⁶	1.08 (1.03-1.13)	1.40E-03

*CI = Confidence interval; HR = Hazard ratio; SD = Standard Deviation; TMR = T-wave morphology restitution; CKD, Chronic kidney disease

Hypertensive Stage 1 defined as 130 mmHg ≤ SBP < 140 mmHg or 85 mmHg ≤ DBP < 90 mmHg

Hypertensive Stage 2 defined as SBP ≥ 140 mmHg or DBP ≥ 90 mmHg

Reference Hypertension group is Hypertensive Stage 0, defined as SBP < 130 mmHg and DBP < 85 mmHg

The ischemic event group (N = 1,424) included individuals with an ICD 10 code I21-I25 for cause of death or admission to hospital.

The non-ischemic event group (N = 319) included individuals in the CV event group with no ischemic event

Supplemental Table 5B: Association with non-ischemic events

	Univariate		Multivariate	
	HR (95% CI)	p	HR (95% CI)	p
Clinical Variables				
Age [per 1 SD]	2.22 (1.92-2.56)	<2x10-16	2.08 (1.81-2.41)	<2x10-16
Sex (male)	1.98 (1.58-2.49)	5.20E-09	2.00 (1.59-2.53)	5.50E-09
Diabetes (yes)	2.35 (1.58-3.48)	2.30E-05	1.25 (0.82-1.88)	3.00E-01
BMI [per 1 SD]	1.27 (1.15-1.40)	1.70E-06	1.21 (1.09-1.35)	6.00E-04
Hypertensive Stage 1	1.73 (1.24-2.43)	1.40E-03	1.18 (0.84-1.66)	3.40E-01
Hypertensive Stage 2	2.21 (1.67-2.94)	4.40E-08	1.14 (0.84-1.53)	4.00E-01
CKD (yes)	9.53 (2.37-38.29)	1.50E-03	7.06 (1.75-28.49)	6.00E-03
ECG variables				
Resting heart rate [per 1 SD]	1.20 (1.10-1.31)	2.70E-05	1.01 (0.90-1.14)	8.50E-01
Heart rate response to exercise [per 1 SD]	0.66 (0.58-0.75)	1.80E-11	1.03 (0.88-1.21)	7.30E-01
Heart rate response to recovery [per 1 SD]	0.71 (0.66-0.75)	<2x10-16	0.88 (0.77-1.02)	9.00E-02
Corrected QT [per 1 SD]	1.19 (1.14-1.25)	3.70E-13	1.15 (1.08-1.22)	9.60E-06
TMR during exercise [per 1 SD]	1.26 (1.16-1.36)	9.60E-09	1.06 (0.96-1.18)	2.20E-01
TMR during recovery [per 1 SD]	1.33 (1.24-1.43)	2.90E-14	1.20 (1.11-1.30)	4.10E-06

*CI = Confidence interval; HR = Hazard ratio; SD = Standard Deviation; TMR = T-wave morphology restitution; CKD, Chronic kidney disease

Hypertensive Stage 1 defined as 130 mmHg ≤ SBP < 140 mmHg or 85 mmHg ≤ DBP < 90 mmHg

Hypertensive Stage 2 defined as SBP ≥ 140 mmHg or DBP ≥ 90 mmHg

Reference Hypertension group is Hypertensive Stage 0, defined as SBP < 130 mmHg and DBP < 85 mmHg

The ischemic event group (N = 1,424) included individuals with an ICD 10 code I21-I25 for cause of death or admission to hospital.

The non-ischemic event group (N = 319) included individuals in the CV event group with no ischemic event

Supplemental Table 6: Association with all-cause mortality

	Univariate		Multivariate	
	HR (95% CI)	p	HR (95% CI)	p
Clinical Variables				
Age [per 1 SD]	2.07 (1.91-2.24)	<2x10⁻¹⁶	1.96 (1.81-2.13)	<2x10⁻¹⁶
Sex (male)	1.76 (1.54-2.00)	<2x10⁻¹⁶	1.60 (1.40-1.83)	3.60E-12
Diabetes (yes)	2.05 (1.62-2.58)	1.70E-09	1.30 (1.03-1.65)	2.80E-02
High cholesterol (yes)	1.52 (1.28-1.80)	2.10E-06	0.92 (0.77-1.10)	3.6x10 ⁻¹
BMI [per 1 SD]	1.08 (1.02-1.15)	9.70E-03	0.99 (0.93-1.06)	8.10E-01
Hypertensive Stage 1	1.35 (1.12-1.64)	2.10E-03	1.00 (0.82-1.21)	9.90E-01
Hypertensive Stage 2	1.88 (1.61-2.20)	1.20E-15	1.12 (0.95-1.32)	1.80E-01
Previous or current smoker (yes)	1.88 (1.65-2.14)	<2x10⁻¹⁶	1.59 (1.39-1.81)	3.80E-12
ECG variables				
Resting heart rate [per 1 SD]	1.18 (1.12-1.24)	7.30E-10	1.15 (1.08-1.22)	1.70E-05
Heart rate response to exercise [per 1 SD]	0.77 (0.72-0.83)	1.50E-12	1.11 (1.03-1.20)	7.00E-03
Heart rate response to recovery [per 1 SD]	0.72 (0.68-0.76)	<2x10⁻¹⁶	0.89 (0.81-0.97)	8.60E-03
Corrected QT [per 1 SD]	1.13 (1.09-1.18)	8.00E-09	1.03 (0.96-1.10)	3.90E-01
QRS duration [per 1 SD]	1.07 (1.01-1.14)	2.80E-02	1.06 (0.99-1.12)	9.10E-02
TMR during exercise [per 1 SD]	1.16 (1.10-1.22)	3.70E-08	1.01 (0.94-1.08)	7.50E-01
TMR during recovery [per 1 SD]	1.26 (1.20-1.32)	<2x10⁻¹⁶	1.10 (1.04-1.17)	1.40E-03

*CI = Confidence interval; HR = Hazard ratio; SD = Standard Deviation; TMR = T-wave morphology restitution

Hypertensive Stage 1 defined as 130 mmHg ≤ SBP < 140 mmHg or 85 mmHg ≤ DBP < 90 mmHg

Hypertensive Stage 2 defined as SBP ≥ 140 mmHg or DBP ≥ 90 mmHg

Reference Hypertension group is Hypertensive Stage 0, defined as SBP < 130 mmHg and DBP < 85 mmHg

Supplemental Table 7: Association with ventricular arrhythmic events

	Univariate		Multivariate	
	HR (95% CI)	p	HR (95% CI)	p
Clinical Variables				
Age [per 1 SD]	1.91 (1.61-2.27)	1.00E-13	1.75 (1.48-2.08)	1.60E-10
Sex (male)	2.37 (1.76-3.20)	1.60E-08	2.20 (1.62-2.97)	3.10E-07
Diabetes (yes)	1.81 (1.05-3.12)	3.30E-02	1.08 (0.62-1.90)	7.80E-01
BMI [per 1 SD]	1.17 (1.03-1.33)	1.70E-02	1.07 (0.92-1.24)	3.70E-01
Hypertensive Stage 1	1.32 (0.84-2.06)	2.20E-01	0.95 (0.61-1.50)	8.40E-01
Hypertensive Stage 2	2.20 (1.55-3.13)	9.70E-06	1.27 (0.88-1.84)	2.00E-01
ECG variables				
HR response to exercise [per 1 SD]	0.73 (0.62-0.85)	6.80E-05	1.08 (0.92-1.26)	3.50E-01
Heart rate response to recovery [per 1 SD]	0.71 (0.65-0.78)	6.60E-14	0.82 (0.69-0.97)	2.10E-02
Corrected QT [per 1 SD]	1.13 (1.03-1.25)	1.10E-02	1.08 (0.96-1.22)	2.00E-01
TMR during exercise [per 1 SD]	1.13 (1.00-1.27)	4.70E-02	0.97 (0.84-1.13)	7.30E-01
TMR during recovery [per 1 SD]	1.28 (1.16-1.41)	1.30E-06	1.16 (1.03-1.30)	1.40E-02

*CI = Confidence interval; HR = Hazard ratio; SD = Standard Deviation; TMR = T-wave morphology restitution; CKD = Chronic kidney disease

Hypertensive Stage 1 defined as 130 mmHg ≤ SBP < 140 mmHg or 85 mmHg ≤ DBP < 90 mmHg

Hypertensive Stage 2 defined as SBP ≥ 140 mmHg or DBP ≥ 90 mmHg

Reference Hypertension group is Hypertensive Stage 0, defined as SBP < 130 mmHg and DBP < 85 mmHg

Supplemental Table 8: Association with atrial fibrillation

	Univariate		Multivariate	
	HR (95% CI)	p	HR (95% CI)	p
Clinical Variables				
Age [per 1 SD]	2.72 (2.50-2.95)	<2x10⁻¹⁶	2.58 (2.37-2.80)	<2x10⁻¹⁶
Sex (male)	2.35 (2.07-2.66)	<2x10⁻¹⁶	2.19 (1.92-2.49)	<2x10⁻¹⁶
Diabetes (yes)	1.69 (1.33-2.14)	1.40E-05	0.92 (0.72-1.18)	5.10E-01
High cholesterol (yes)	1.68 (1.44-1.96)	7.90E-11	0.90 (0.77-1.05)	1.90E-01
BMI [per 1 SD]	1.28 (1.21-1.35)	<2x10⁻¹⁶	1.24 (1.17-1.32)	1.60E-12
Hypertensive Stage 1	1.38 (1.15-1.67)	6.10E-04	0.89 (0.74-1.08)	2.30E-01
Hypertensive Stage 2	2.21 (1.91-2.57)	<2x10⁻¹⁶	1.05 (0.90-1.22)	5.70E-01
Previous or current smoker (yes)	1.40 (1.24-1.57)	3.30E-08	1.08 (0.96-1.22)	1.90E-01
CKD (yes)	3.92 (1.26-12.16)	1.80E-02	3.08 (0.99-9.57)	5.20E-02
ECG variables				
Heart rate response to exercise [per 1 SD]	0.65 (0.61-0.70)	<2x10⁻¹⁶	0.97 (0.88-1.06)	4.70E-01
Heart rate response to recovery [per 1 SD]	0.72 (0.69-0.75)	<2x10⁻¹⁶	0.92 (0.85-0.99)	2.30E-02
Corrected QT [per 1 SD]	1.15 (1.11-1.19)	1.80E-15	1.12 (1.07-1.17)	1.70E-07
TMR during exercise [per 1 SD]	1.13 (1.08-1.19)	7.20E-07	1.01 (0.95-1.08)	7.00E-01
TMR during recovery [per 1 SD]	1.19 (1.13-1.24)	1.30E-12	1.03 (0.98-1.09)	2.80E-01

*CI = Confidence interval; HR = Hazard ratio; SD = Standard Deviation; TMR = T-wave morphology restitution; CKD, Chronic kidney disease

Hypertensive Stage 1 defined as 130 mmHg ≤ SBP < 140 mmHg or 85 mmHg ≤ DBP < 90 mmHg

Hypertensive Stage 2 defined as SBP ≥ 140 mmHg or DBP ≥ 90 mmHg

Reference Hypertension group is Hypertensive Stage 0, defined as SBP < 130 mmHg and DBP < 85 mmHg

Supplemental Table 9: Genome-wide significant SNVs for TMR during exercise and during recovery in the discovery sample

Trait	Chr	Pos	SNV	EA	AA	EAF	β	SE	P	N
TMR during exercise	11	2484803	rs2074238	T	C	0.090	0.073	13	1.10E-08	293
TMR during recovery	1	1620152	rs10918571	A	G	0.751	0.042	07	1.40E-08	288
TMR during recovery	1	1620157	rs12036340	A	G	0.751	0.042	07	1.40E-08	288
TMR during recovery	1	1620210	rs2010491	A	G	0.758	0.042	08	2.00E-08	284
TMR during recovery	1	1620212	rs146475167	A	G	0.757	0.042	08	2.30E-08	283
TMR during recovery	1	1620231	rs60129000	T	C	0.756	0.042	07	1.50E-08	289
TMR during recovery	1	1620242	rs12042862	C	T	0.756	0.042	07	1.80E-08	289
TMR during recovery	1	1620338	rs12143842	C	T	0.752	0.043	07	8.10E-09	290
TMR during recovery	1	1621331	rs12029454	G	A	0.861	0.051	09	3.80E-08	290
TMR during recovery	1	1621341	rs12033217	C	A	0.862	0.051	09	4.20E-08	290
TMR during recovery	11	2478519	rs12271931	G	A	0.139	0.087	10	7.70E-19	259
TMR during recovery	11	2484803	rs2074238	T	C	0.090	0.131	11	1.40E-31	290
TMR during recovery	11	2505436	rs117903261	C	T	0.973	0.191	21	2.40E-19	249
TMR during recovery	11	2510418	rs7115906	T	C	0.032	0.114	19	8.00E-10	279

TMR during								0.0	3.70E-	253
recovery	11	2520974	rs79888274	G	A	0.904	0.077	12	11	98
TMR during		2456193						0.0	3.40E-	273
recovery	12	8	rs10771085	C	T	0.430	0.042	07	10	68
TMR during		2456434						0.0	1.20E-	278
recovery	12	4	rs7955427	T	C	0.621	0.041	07	09	81
TMR during		2456610						0.0	1.50E-	277
recovery	12	5	rs4309241	T	C	0.451	0.042	07	10	55
TMR during		2456611						0.0	4.10E-	279
recovery	12	4	rs4505147	C	A	0.649	0.041	07	09	14
TMR during		2456612						0.0	1.60E-	277
recovery	12	3	rs4517618	C	T	0.451	0.042	07	10	41
TMR during		2456768						0.0	2.70E-	280
recovery	12	3	rs11047427	C	G	0.649	0.041	07	09	56
TMR during		2456822						0.0	6.80E-	279
recovery	12	2	rs10771086	C	T	0.451	0.043	07	11	34
TMR during		2457156						0.0	2.50E-	283
recovery	12	1	rs11047430	G	A	0.635	0.040	07	09	78
TMR during		2457395	12:24573951_AG					0.0	6.40E-	283
recovery	12	1	_A	AG	A	0.634	0.039	07	09	64
TMR during		2457685						0.0	3.10E-	283
recovery	12	9	rs1396206	A	T	0.480	0.048	07	13	18
TMR during		2457907						0.0	5.80E-	285
recovery	12	9	rs10842343	A	T	0.607	0.041	07	10	49
TMR during		2458140						0.0	5.80E-	284
recovery	12	4	rs4488295	T	C	0.462	0.043	07	11	80
TMR during		2458236						0.0	5.20E-	285
recovery	12	7	rs10842344	T	C	0.462	0.043	07	11	03
TMR during		2458565						0.0	5.10E-	286
recovery	12	4	rs1973564	A	G	0.480	0.043	06	11	69
TMR during		2458639						0.0	3.70E-	288
recovery	12	0	rs4963759	A	T	0.505	0.047	06	13	52

TMR during		2458749						0.0	1.50E-	288
recovery	12	1	rs11047436	T	A	0.665	0.039	07	08	75
TMR during		2458870						0.0	6.90E-	287
recovery	12	9	rs10771089	C	G	0.480	0.042	06	11	15
TMR during		2458874						0.0	5.90E-	287
recovery	12	9	rs10771090	A	G	0.523	0.047	07	13	17
TMR during		2458915						0.0	6.40E-	287
recovery	12	1	rs2900532	C	A	0.480	0.042	06	11	20
TMR during		2459040						-	0.0	4.30E-
recovery	12	5	rs11047438	G	A	0.540	0.043	06	11	35
TMR during		2459208						0.0	4.70E-	289
recovery	12	7	rs11047439	C	T	0.662	0.040	07	09	42
TMR during		2459362						0.0	6.20E-	289
recovery	12	4	rs11047441	C	G	0.660	0.040	07	09	61
TMR during		2459519						0.0	3.70E-	289
recovery	12	2	rs7307613	C	T	0.503	0.047	06	13	80
TMR during		2459639						-	0.0	3.70E-
recovery	12	1	rs7297742	T	G	0.540	0.043	06	11	13
TMR during		2459900						0.0	4.10E-	289
recovery	12	5	rs11047444	A	G	0.661	0.040	07	09	67
TMR during		2459957						0.0	3.30E-	289
recovery	12	8	rs10842350	A	G	0.504	0.047	06	13	76
TMR during		2460104						0.0	3.70E-	289
recovery	12	8	rs11047447	A	G	0.661	0.040	07	09	70
TMR during		2460181						0.0	3.50E-	289
recovery	12	8	rs11047449	T	C	0.462	0.043	06	11	78
TMR during		2460242						0.0	4.00E-	289
recovery	12	1	rs1396197	G	A	0.663	0.040	07	09	59
TMR during		2460287						0.0	4.10E-	289
recovery	12	3	rs1396198	T	C	0.662	0.040	07	09	64
TMR during		2460313						0.0	4.40E-	289
recovery	12	0	rs11047451	A	T	0.663	0.040	07	09	54

TMR during		2460722					-	0.0	3.20E-	289
recovery	12	5	rs1508224	C	T	0.539	0.043	06	11	48
TMR during		2461294						0.0	3.30E-	289
recovery	12	4	rs2136019	C	T	0.463	0.043	06	11	63
TMR during		2461436						-	0.0	3.80E-
recovery	12	5	rs4465447	C	A	0.494	0.047	06	13	55
TMR during		2461448						-	0.0	3.60E-
recovery	12	6	rs4259904	A	G	0.494	0.047	06	13	52
TMR during		2461511						-	0.0	4.80E-
recovery	12	4	rs10842353	G	A	0.320	0.038	07	08	37
TMR during		2461620						0.0	8.70E-	289
recovery	12	9	rs7957437	C	A	0.508	0.046	06	13	40
TMR during		2461725	12:24617257_ATT					-	0.0	4.60E-
recovery	12	7	_A	ATT	A	0.291	0.041	07	08	20
TMR during		2461765						-	0.0	3.70E-
recovery	12	9	rs11047460	T	C	0.494	0.047	06	13	27
TMR during		2462079						0.0	1.10E-	290
recovery	12	1	rs4403889	A	G	0.462	0.044	06	11	13
TMR during		2462096						0.0	1.10E-	290
recovery	12	9	rs4376999	A	G	0.462	0.044	06	11	00
TMR during		2462134						0.0	1.00E-	289
recovery	12	8	rs10842356	A	T	0.485	0.042	06	10	93
TMR during		2462203						0.0	2.30E-	289
recovery	12	6	rs4963761	C	T	0.514	0.045	06	12	67
TMR during		2462216						0.0	1.00E-	289
recovery	12	0	rs4963762	T	C	0.462	0.044	06	11	92
TMR during		2462361						0.0	1.10E-	289
recovery	12	8	rs7299141	A	G	0.462	0.044	06	11	90
TMR during		2462843						0.0	2.10E-	289
recovery	12	3	rs10842357	T	G	0.461	0.043	06	11	29
TMR during		2462893						0.0	3.60E-	278
recovery	12	2	rs146081992	A	T	0.517	0.036	07	08	33

TMR during		2462893			A			0.0	3.60E-	278
recovery	12	8	rs368370337	A	T	0.517	0.036	07	08	33
TMR during		2463031						0.0	3.20E-	289
recovery	12	5	rs4963764	A	G	0.461	0.043	06	11	03
TMR during		2463253						0.0	5.90E-	288
recovery	12	8	rs10771091	C	T	0.461	0.042	06	11	94
TMR during		2463333						0.0	5.60E-	288
recovery	12	2	rs4441108	A	T	0.461	0.042	06	11	94
TMR during		2463430						0.0	1.70E-	288
recovery	12	6	rs10771092	T	C	0.489	0.044	06	11	96
TMR during		2464085						0.0	1.70E-	289
recovery	12	5	rs7970266	T	C	0.461	0.041	06	10	05
TMR during		2464203						0.0	2.00E-	288
recovery	12	4	rs10842358	C	T	0.461	0.041	06	10	95
TMR during		2464398	12:24643986_CT	CTC				0.0	3.70E-	286
recovery	12	6	CTT_C	TT	C	0.462	0.041	07	10	71
TMR during		2464901						0.0	1.50E-	288
recovery	12	3	rs7961520	T	C	0.451	0.039	06	09	86
TMR during		2465637						0.0	1.90E-	288
recovery	12	5	rs10842362	C	T	0.450	0.039	06	09	81
TMR during		2465754						0.0	4.40E-	288
recovery	12	7	rs7295036	A	G	0.436	0.041	07	10	62
TMR during		2465880	12:24658806_TG					0.0	2.70E-	284
recovery	12	6	C_T	TGC	T	0.448	0.044	07	11	03
					A					
					A					
					G					
TMR during		2465935			A			0.0	1.30E-	286
recovery	12	2	rs559214768	A	G	0.439	0.042	07	10	22
TMR during		2465996						0.0	1.60E-	286
recovery	12	2	rs7304608	G	A	0.451	0.039	07	09	67
TMR during		2465997						0.0	2.60E-	287
recovery	12	5	rs7304397	C	T	0.433	0.041	07	10	71

TMR during		2465998						0.0	2.60E-	287
recovery	12	2	rs7304404	C	T	0.433	0.041	07	10	71
TMR during		2466603						0.0	1.70E-	290
recovery	12	9	rs10743500	T	C	0.437	0.041	06	10	13
TMR during		2466615						0.0	2.10E-	289
recovery	12	5	rs4275708	C	T	0.449	0.039	06	09	50
TMR during		2466716						0.0	3.90E-	288
recovery	12	4	rs4614552	T	G	0.616	0.037	07	08	07
TMR during		2466760						0.0	3.20E-	288
recovery	12	1	rs10743501	C	T	0.434	0.041	06	10	89
TMR during		2466910						-	0.0	2.80E-
recovery	12	1	rs4439602	C	T	0.554	0.039	07	09	43
TMR during		2466910						0.0	2.70E-	286
recovery	12	2	rs2970418	G	A	0.448	0.039	07	09	55
TMR during		2467100						0.0	5.60E-	276
recovery	12	7	rs374287296	CT	C	0.466	0.038	07	09	09
TMR during		2467209						0.0	7.70E-	285
recovery	12	4	rs2955487	G	C	0.441	0.040	07	10	54
TMR during		2467343						-	0.0	3.00E-
recovery	12	7	rs11397830	T	A	0.544	0.039	07	09	59
TMR during		2467522						0.0	5.00E-	284
recovery	12	2	rs2970419	C	A	0.457	0.038	07	09	51
TMR during		2467547						0.0	1.10E-	283
recovery	12	9	rs7296354	A	G	0.541	0.037	07	08	68

*TMR: T-wave morphology restitution, SNV: single-nucleotide variant, Chr: Chromosome, Pos: Position, based on HG build 18, EA: Effect allele, AA: Alternate allele, EAF: Effect allele frequency, β : Beta, SE: Standard Error, N: number of participants, *P*: P-value.

Supplemental Table 10A: Lookup of loci associated with TMR during exercise in the MTAG

results

Locus	SNV	CHR	BP	EA	EAF	Discovery				Replication				Combined				MTAG					
						P	N	β	SE	P	N	β	SE	P	N	β	SE	P	N	β	SE		
RNF207	rs709208	1	6272137	A	0.0679	2.67	0.00	0.00	0.00	1.60	0.00	0.00	0.00	1.89	0.00	0.00	0.00	9.09	0.00	0.00	0.00		
						0E	9	0	0	0E	7	0	0	0E	2	0	0	5E	2	0	0	0	0
						-	3	4	0	-	6	4	0	-	0	4	0	-	0	4	0	-	0
NOS1AP**	rs12143842	1	162033890	C	0.0570	1.29	0.00	0.00	0.00	3.41	0.00	0.00	0.00	6.61	0.00	0.00	0.00	2.01	0.00	0.00	0.00		
						0E	3	0	0	0E	8	0	0	0E	7	0	0	1E	7	0	0	0	0
						-	9	3	0	-	5	2	1	-	6	3	0	-	6	4	0	-	6
SCN5A-SCN10A^A	rs7428232	3	1878618	T	0.0416	5.29	0.00	0.00	0.00	1.81	0.00	0.00	0.00	3.71	0.00	0.00	0.00	2.01	0.00	0.00	0.00		
						0E	3	0	0	0E	8	0	0	0E	6	0	0	2E	6	0	0	0	0
						-	5	3	0	-	2	3	0	-	9	3	0	-	9	3	0	-	9
PREP"	rs4478445	6	105786660	C	0.0430	2.58	0.00	0.00	0.00	7.41	0.00	0.00	0.00	8.00	0.00	0.00	0.00	4.20	0.00	0.00	0.00		
						0E	9	0	0	0E	4	0	0	0E	9	0	0	7E	9	0	0	0	0
						-	1	6	1	-	9	4	1	-	1	5	1	-	1	6	1	-	1
KCNH2	rs2072412	7	150647970	C	0.029	1.88	0.00	0.00	0.00	4.11	0.00	0.00	0.00	2.11	0.00	0.00	0.00	1.41	0.00	0.00	0.00		
						0E	9	0	0	0E	5	0	0	0E	0	0	0	2E	0	0	0	0	0
						-	7	4	0	-	3	4	1	-	2	4	0	-	2	4	0	-	2
KCNQ1*	rs2074238	1	2484803	T	0.088	1.19	0.00	0.00	0.00	1.21	0.00	0.00	0.00	1.21	0.00	0.00	0.00	7.01	0.00	0.00	0.00		
						0E	3	0	0	0E	8	0	0	0E	7	0	0	2E	7	1	0	0	0
						-	9	7	1	-	5	4	1	-	6	6	1	-	6	2	1	-	6
SOX5*	rs7307613	1	24595192	C	0.055	1.89	0.00	0.00	0.00	3.51	0.00	0.00	0.00	2.81	0.00	0.00	0.00	3.51	0.00	0.00	0.00		
						0E	3	0	0	0E	8	0	0	0E	7	0	0	7E	7	0	0	0	0
						-	5	3	0	-	2	3	0	-	0	3	0	-	0	5	0	-	0
KCNJ2‡	17:68493468_GA_G	1	68493468	G	0.077	7.69	0.00	0.00	0.00	3.71	0.00	0.00	0.00	2.91	0.00	0.00	0.00	9.91	0.00	0.00	0.00		
						0E	3	0	0	0E	7	0	0	0E	6	0	0	7E	5	0	0	0	0
						-	1	3	0	-	9	4	0	-	3	4	0	-	4	3	0	-	4

SNV: single-nucleotide variation, CHR: Chromosome, BP: Position, based on HG build 19, EA: Effect allele, EAF: Effect allele frequency from discovery data, β : Beta, SE: Standard Error, N: number of participants, P: P-value. The locus name indicates the coding gene that is in the closest proximity to the most associated SNV. The loci labelled as TSC22D2 and KCNJ2 have a lncRNA and a pseudogene as the nearest. Replicated SNPs are indicated in bold type. * indicates the SNP is the same or in high LD ($r^2 > 0.8$) with a SNP associated with the other index. ^ indicates has a secondary signal. " indicates identified with MTAG. ‡ A proxy (rs1860452) was used for this SNV with MTAG (LD > 0.95)

Supplemental Table 10B: Lookup of loci associated with TMR during exercise in the MTAG

results

Locus	SNV	C H R	BP	E A	E A F	Discovery				Replication				Combined				MTAG				
						P	N	β	SE	P	N	β	SE	P	N	β	SE	P	N	β	SE	
							2				2				4				4			
SSBP	rs56		547		0.		8	0.	0.		1	0.	0.		9	0.	0.		9	0.	0.	
	240		426		4	6.2	2	0	0	7.4	0	0	0	3.7	8	0	0	1.8	8	0	0	
	3	8	18	A	0	0E	9	3	0	0E	9	2	0	0E	9	2	0	5E	9	3	0	
							-06	9	0	7	-03	1	0	8	-08	5	7	5	-08	5	5	6
							2	-			2	-			5	-			5	-		
					0.		9	0.	0.		1	0.	0.		1	0.	0.		1	0.	0.	
NOS1 AP*	rs12		162		7	8.1	0	0	0	1.6	6	0	0	5.1	1	0	0	5.2	1	0	0	
	143		033		5	0E	1	4	0	0E	2	4	0	0E	5	4	0	9E	5	5	0	
	842	1	890	C	0	-09	3	3	7	-08	3	8	9	-16	3	5	6	-17	3	9	7	
							2				2				4				4			
SCN5					0.		6	0.	0.		0	0.	0.		7	0.	0.		7	0.	0.	
A-	rs73		387		0	2.0	9	1	0	2.1	1	1	0	1.6	5	1	0	6.3	5	1	0	
SCN1	730		103		1	0E	7	1	2	0E	0	3	2	0E	6	2	1	5E	6	6	2	
0A^	65	3	15	T	9	-06	9	4	4	-06	7	2	8	-11	6	2	8	-13	6	5	3	
							2	-			2	-			4	-			5	-		
					0.		7	0.	0.		0	0.	0.		9	0.	0.		0	0.	0.	
TSC2	rs11		149		8	1.4	8	0	0	5.3	7	0	0	9.3	1	0	0	6.6	4	0	0	
	271		943		6	0E	5	4	1	0E	6	3	1	0E	1	4	0	9E	3	5	0	
	715		115	G	3	-06	7	6	0	-03	2	1	1	-09	5	1	7	-09	9	2	9	
2D2‡	4	3				2	-				2	-			5	-			5	-		
					0.		8	0.	0.		1	0.	0.		0	0.	0.		0	0.	0.	
CAMK	rs35		114		7	6.2	3	0	0	1.4	1	0	0	2.9	0	0	0	2.1	9	0	0	
	408		423		3	0E	6	2	0	0E	3	4	0	0E	0	3	0	8E	8	3	0	
	2D‡	611	4	677	C	8	-03	2	0	7	-08	8	8	8	-08	6	1	6	-07	8	6	7
							2	-			2	-			5	-			5	-		
					0.		9	0.	0.		1	0.	0.		1	0.	0.		1	0.	0.	
KCNQ	rs20		248		0	1.4	0	1	0	4.2	6	1	0	1.2	1	1	0	5.0	1	1	0	
	742	1	480		8	0E	1	3	1	0E	2	5	1	0E	5	3	0	6E	5	7	1	
	1*	38	1	3	T	8	-31	3	1	1	-31	3	2	3	-59	3	8	8	-58	3	4	1
							2				2				4				4			
					0.		8	0.	0.		1	0.	0.		9	0.	0.		9	0.	0.	
SOX5	rs13		245		4	3.1	3	0	0	4.0	1	0	0	1.3	9	0	0	4.9	9	0	0	
	962	1	768		8	0E	1	4	0	0E	0	3	0	0E	2	4	0	1E	2	5	0	
	* 06	2	59	A	2	-13	8	8	7	-05	5	1	7	-16	7	0	5	-19	7	5	6	
							2	-			2	-			5	-			5	-		
					0.		8	0.	0.		1	0.	0.		0	0.	0.		0	0.	0.	
KLF12	rs79		745		6	2.5	9	0	0	6.0	5	0	0	6.4	9	0	0	2.7	9	0	0	
	923	1	093		3	0E	0	3	0	0E	4	2	0	0E	6	2	0	0E	6	3	0	
	" 14	3	46	G	1	-06	8	2	7	-03	5	1	8	-08	8	7	5	-08	8	5	6	

SNV: single-nucleotide variation, CHR: Chromosome, BP: Position, based on HG build 19, EA: Effect allele, EAF: Effect allele frequency from discovery data, β: Beta, SE: Standard Error, N: number of participants, P: P-value. The locus name indicates the coding gene that is in the closest proximity to the most associated SNV. The loci labelled as TSC22D2 and KCNJ2 have a LncRNA and a pseudogene as the nearest. Replicated SNPs are indicated in bold type. * indicates the SNP is the same or in high LD ($r^2>0.8$) with a SNP associated with the other index. ^ indicates has a secondary signal. " indicates identified with MTAG. ‡ A proxy was used for the SNV at TSC22D2 (rs2867860, LD>0.95) and for the SNV at CAMK2D (rs4834342, LD>0.95) for MTAG.

Supplemental Table 11A: TMR during exercise loci associations with other traits using PhenoScanner v2

Locus	Lead SNV	Proxy SNV	Proxy Chr:Pos (hg19)	EA	r2	Type	Trait	P	PMID	
NOS1AP	rs12143842	rs12036340	chr1:162015740	A/	0.94	9	Proxy	QRS complex 12-leads	1.00E-09	27659466
				G/						
	rs12143842	rs12143842	chr1:162033890	T	1	Lead	Arrhythmias cardiac	1.00E-83	19587794	
				C/						
rs12143842	rs12143842	chr1:162033890	T	1	Lead	Electrocardiography	2.00E-78	19305408		
			C/							
rs12143842	rs12143842	chr1:162033890	T	1	Lead	QT interval	1.00E-213	24952745		
			C/							
SCN5A-					0.87					
SCN10A	rs7373065	rs6773331	chr3:38684397	T/A	9	Proxy	Pulse rate	8.05E-09	100000001	
				C/						
rs7373065	rs7373065	chr3:38710315	T	1	Lead	Cause of death: cardiomegaly	2.69E-08	100000001		
			G/							
rs7428232	rs10428132	chr3:38777554	T	6	Proxy	Brugada syndrome	1.00E-68	23872634		
			C/							
rs7428232	rs6599255	chr3:38796415	A	4	Proxy	Resting heart rate	2.00E-10	27798624		
			G/							
rs7428232	rs6790396	chr3:38771925	C	6	Proxy	P wave duration	2.00E-39	28794112		
			G/							
rs7428232	rs6795970	chr3:38766675	A	4	Proxy	conduction measures	5.00E-27	23463857		
			G/							
rs7428232	rs6795970	chr3:38766675	A	4	Proxy	Electrocardiographic traits	1.00E-58	20062063		
			T/							
rs7428232	rs6800541	chr3:38774832	C	6	Proxy	Electrocardiography	2.00E-74	20062060		
			T/							
rs7428232	rs6800541	chr3:38774832	C	6	Proxy	PR interval	9.70E-82	20062060		
			C/							
rs7428232	rs6801957	chr3:38767315	T	4	Proxy	Heart function tests	3.00E-14	21076409		
			C/							
rs7428232	rs6801957	chr3:38767315	T	4	Proxy	Pulse rate	2.98E-13	100000001		
			C/							
rs7428232	rs6801957	chr3:38767315	T	4	Proxy	QRS duration	7.00E-40	27659466		
			C/							
rs7428232	rs6801957	chr3:38767315	T	4	Proxy	QT interval	1.00E-10	24952745		
			C/							
PREP	rs4478445	rs67125925	chr6:105780309	T	1	Proxy	Pulse rate	8.90E-10	100000001	
KCNH2	rs2072412	rs2072413	chr7:150647969	T/	1	Proxy	QT interval	1.00E-49	24952745	
				C/						
KCNQ1	rs2074238	rs2074238	chr11:2484803	T	1	Lead	Electrocardiography	3.00E-17	19305408	
				C/						
rs2074238	rs2074238	chr11:2484803	T	1	Lead	QT interval	2.00E-28	24952745		
			C/							
KCNJ2	rs17779747	rs17779747	chr17:68494992	T	1	Lead	Electrocardiography	6.00E-12	19305409	

			G/						
rs17779747	rs17779747	chr17:68494992	T	1	Lead	QT interval	6.00E-12	19305409	

* The look-up results from the lead TMR SNV or proxy SNVs in high LD ($r^2 \geq 0.8$) from the 1000 Genome Project are indicated. SNVs are ordered by chromosomal position, and only results with P value $\leq 5 \times 10^{-8}$ are included. If there were multiple results for the same trait, the variant with the lowest P-value is shown. Proxy variants with additional traits that were not associated with the lead variants are also included. If multiple proxy SNVs were available, the proxy SNV with the highest LD was chosen. EA: Effect allele; r^2 : A measure of the linkage disequilibrium between the proxy and lead SNV; Type: Whether the variant is the lead or proxy variant; P: P-value for the association between the variant and the trait; PMID: PubMed ID. The locus name indicates the coding gene that is in the closest proximity to the most associated SNV. The loci labelled as TSC22D2 and KCNJ2 have a LncRNA and a pseudogene as the nearest. Phenoscanner v2 (PMID: 27318201).

Supplemental Table 11B: TMR during recovery loci associations with other traits using PhenoScanner v2

Locus	Lead SNV	Proxy SNV	Proxy Chr:Pos (hg19)	EA	r ²	Type	Trait	P	PMID
<i>NOS1AP</i>	rs12143842	rs12036340	chr1:162015740	A/G	0.94	Prox	QRS complex 12-leads	1.00E-09	27659466
	rs12143842	rs12143842	chr1:162033890	C/T	9	y	Arrhythmias cardiac	1.00E-83	19587794
	rs12143842	rs12143842	chr1:162033890	C/T	1	Lead	Electrocardiographic traits	4.00E-18	25055868
	rs12143842	rs12143842	chr1:162033890	C/T	1	Lead	Electrocardiography	2.00E-78	19305408
	rs12143842	rs12143842	chr1:162033890	C/T	1	Lead	QT interval	1.00E-213	24952745
<i>SSBP3</i>	rs562408	rs562408	chr1:54742618	A/G	1	Lead	P wave duration	3.00E-09	28794112
<i>SCN5A-</i>							Cause of death:		
<i>SCN10A</i>	rs7373065	rs7373065	chr3:38710315	C/T	1	Lead	cardiomegaly	2.69E-08	100000001
	rs9311197	rs10428132	chr3:38777554	T/G	0.80	Prox	Brugada syndrome	1.00E-68	23872634
	rs9311197	rs10428132	chr3:38777554	T/G	0.80	Prox	Pulse rate	3.52E-13	100000001
	rs9311197	rs6790396	chr3:38771925	G	0.80	Prox	PR interval	2.18E-08	21347284
	rs9311197	rs6790396	chr3:38771925	G	0.80	Prox	P wave duration	2.00E-39	28794112
	<i>KCNQ1</i>	rs2074238	rs2074238	chr11:2484803	C/T	1	Lead	Electrocardiography	3.00E-17
rs2074238		rs2074238	chr11:2484803	C/T	1	Lead	QT interval	2.00E-28	24952745
<i>KLF12</i>	rs7992314	rs1886512	chr13:74520186	A/T	0.97	Prox	Heart function tests	1.00E-08	21076409
	rs7992314	rs728926	chr13:74513122	T/C	0.98	Prox	QRS duration	6.00E-11	27659466
	rs7992314	rs728926	chr13:74513122	T/C	0.98	Prox	QT interval	2.00E-08	24952745

* The look-up results from the lead TMR SNV or proxy SNVs in high LD ($r^2 \geq 0.8$) from the 1000 Genome Project are indicated. SNVs are ordered by chromosomal position, and only results with P value $\leq 5 \times 10^{-8}$ are included. If there were multiple results for the same trait, the variant with the lowest P-value is shown. Proxy variants with additional traits that were not associated with the lead variants are also included. If multiple proxy SNVs were available, the proxy SNV with the highest LD was chosen. EA: Effect allele; r²: A measure of the linkage disequilibrium between the proxy and lead SNV; Type: Whether the variant is the lead or proxy variant; P: P-value for the association between the variant and the trait; PMID: PubMed ID. The locus name indicates the coding gene that is in the closest proximity to the most

associated SNV. The loci labelled as TSC22D2 and KCNJ2 have a LncRNA and a pseudogene as the nearest. Phenoscanner v2 (PMID: 27318201).

Supplementary Table 12: Expression quantitative trait locus (eQTL) analysis for TMR during exercise and recovery traits

Lead SNV	Marker	Locus	Proxy SNV	Proxy SNV Chr:Pos (hg19)	Top eQTL SNV	r ² (Lead SNV-proxy SNV)	r ² (Lead SNV-Top eQTL SNV)	SNV (P)	Top eQTL SNV (P)	Tissue	Transcript
rs12143842	TMRex and TMRrec	NO S1 AP	rs12143842	chr1:162024242	rs12143842	1.000	1.000	4.70E-12	4.70E-12	Heart atrial appendage	C1orf226
rs562408	TMRrec	SS BP3	rs562408	chr1:54742618	rs562408	1.000	1.000	6.80E-23	6.80E-23	Heart atrial appendage	SSBP3

*TMR during exercise and recovery variants with significant eQTLs and their corresponding genes are indicated. The results from proxy variants, with high LD ($r^2 \geq 0.8$) with the lead variant in the UK Biobank study were included if there was tissue expression data in addition to the lead variant. Results were filtered to those reaching a P value $\leq 5 \times 10^{-8}$. The source was Genotype-Tissue Expression (GTEx) Consortium, PubMed ID is 25954001. r^2 : A measure for the linkage disequilibrium between the proxy and lead SNVs; P : P value for the association between the variant and RNA tissue expression. The locus name indicates the coding gene that is in the closest proximity to the most associated SNV. The loci labelled as *TSC22D2* and *KCNJ2* have a LncRNA and a pseudogene as the nearest.

Supplemental Table 13: Long-range interactors in heart, adrenal, brain tissue and neural progenitor cells

Locus	Lead SNV	Proxy SNV	r2	Marker	Score	Right Ventricle	Left Ventricle	Hippocampus	Neural Progenitor Cell	Aorta
<i>SSBP3</i>	rs562408	rs702496	0.835	TMRrec	5		<i>SSBP3</i>			
	rs562408	rs1537430	0.949	TMRrec	5		<i>SSBP3</i>			
	rs562408	rs3753410	0.812	TMRrec	5		<i>SSBP3</i>			
	rs562408	rs536684	0.983	TMRrec	4		<i>SSBP3</i>			
	rs562408	rs590041	0.991	TMRrec	5		<i>SSBP3</i>			
	rs562408	rs562408	1.000	TMRrec	5		<i>SSBP3</i>			
<i>NOS1A P</i>	rs12143842	rs12143842	1.000	Both	2b				<i>UHMK1;SH2D1B</i>	<i>SH2D1B</i>
<i>SCN5A-SCN10A</i>	rs7428232	rs6783110	0.865	TMRex	5					
	rs7428232	rs6795970	0.945	TMRex	5		<i>SCN5A</i>			<i>SCN5A</i>
	rs7428232	rs6801957	0.984	TMRex	4		<i>SCN5A</i>			<i>SCN5A</i>
	rs7428232	rs7433306	0.977	TMRex	5		<i>SCN5A</i>			<i>SCN5A</i>
	rs7428232	rs6790396	0.996	TMRex	4		<i>SCN5A</i>			<i>SCN5A</i>
	rs7428232	rs9809798	0.801	TMRex	5		<i>SCN5A</i>			<i>SCN5A</i>
	rs7428232	rs10428132	0.996	TMRex	5		<i>SCN5A</i>			<i>SCN5A</i>
	rs7428232	rs7428167	0.801	TMRex	2b		<i>SCN5A</i>			<i>SCN5A</i>
	rs7428232	rs6599250	0.976	TMRex	5		<i>SCN5A</i>			<i>SCN5A</i>
<i>SCN5A-SCN10A</i>	rs9311197	rs6790396	0.805	sec signal, TMRrec	4		<i>SCN5A</i>			<i>SCN5A</i>
	rs9311197	rs9809798	1.000	sec signal, TMRrec	5		<i>SCN5A</i>			<i>SCN5A</i>
	rs9311197	rs10428132	0.805	sec signal, TMRrec	5		<i>SCN5A</i>			<i>SCN5A</i>
	rs9311197	rs7428167	1.000	sec signal, TMRrec	2b		<i>SCN5A</i>			<i>SCN5A</i>
<i>TSC22D2</i>	rs112717154	rs11923657	0.865	TMRrec	4	<i>TSC22D2</i>	<i>EIF2A;TSC22D2</i>		<i>TSC22D2</i>	<i>TSC22D2</i>
	rs112717154	rs12634526	0.889	TMRrec	4	<i>TSC22D2</i>	<i>EIF2A;TSC22D2</i>		<i>TSC22D2</i>	<i>TSC22D2</i>
<i>PREP</i>	rs4478445	rs55759324	0.984	TMRex	5		<i>ATG5</i>			
	rs4478445	rs60847040	0.984	TMRex	5		<i>ATG5</i>			
	rs4478445	rs58971260	1.000	TMRex	4		<i>PREP</i>			
	rs4478445	rs67558059	0.934	TMRex	4		<i>PREP</i>			
	rs4478445	rs67125925	0.886	TMRex	5		<i>PREP</i>			
	rs4478445	rs66935099	0.934	TMRex	5		<i>PREP</i>			
	rs4478445	rs67092423	0.934	TMRex	5		<i>PREP</i>			
	rs4478445	rs67330396	0.934	TMRex	5		<i>PREP</i>			
	rs4478445	rs60127716	0.934	TMRex	5		<i>PREP</i>			

	rs4478445	rs558 73742	0.934	TMRex	5	<i>PREP</i>	
<i>SOX5</i>	rs1396206	rs139 6206	1.000	TMRrec	5		
	rs1396206	rs440 3889	0.844	TMRrec	5		<i>SOX</i> 5
	rs1396206	rs797 0266	0.819	TMRrec	5	<i>SOX5</i>	<i>SOX</i> 5
	rs1396206	rs108 42358	0.819	TMRrec	5	<i>SOX5</i>	<i>SOX</i> 5
<i>KLF12</i>	rs7992314	rs170 61696	0.996	TMRrec	5	<i>KLF12</i>	<i>KLF</i> 12
	rs7992314	rs728 926	0.988	TMRrec	5	<i>KLF12</i>	<i>KLF</i> 12
	rs7992314	rs957 3330	0.992	TMRrec	5	<i>KLF12</i>	<i>KLF</i> 12
	rs7992314	rs188 6512	0.981	TMRrec	5	<i>KLF12</i>	<i>KLF</i> 12
<i>KCNJ2</i>	17:684934 68_GA_G	rs728 68940	0.836	TMRex	5	<i>CDC42E</i> <i>P4</i>	
	17:684934 68_GA_G	rs721 8368	0.996	TMRex	5	<i>CDC42E</i> <i>P4</i>	
	17:684934 68_GA_G	rs177 80076	0.826	TMRex	5	<i>CDC42E</i> <i>P4</i>	

*Results are presented for all SNVs in LD $r^2 \geq 0.8$ with lead SNVs found in this study that have a functional score ≤ 5 , and the locus has at least one significant Hi-C interaction. The locus name indicates the coding gene that is in the closest proximity to the most associated SNV. The loci labelled as *TSC22D2* and *KCNJ2* have a LncRNA and a pseudogene as the nearest.

Supplemental Table 14. Candidate Genes for g:profiler analysis

Locus	Marker	SNV	CHR	BP	Candidate genes within 5 kb	eQTL	Hi-C interactor genes	Mouse model with cardiovascular or nervous system	Candidate gene(s) at locus
<i>RNF207</i>	TMRex	rs709208	1	6272137	<i>RNF207</i>				<i>RNF207</i>
<i>SSBP3</i>	TMRrec	rs562408	1	54742618	<i>SSBP3</i>	<i>SSBP3</i>	<i>SSBP3</i>	<i>SSBP3</i> (http://www.informatics.jax.org/marker/MGI:1919725)	<i>SSBP3</i>
<i>NOS1AP</i>	TMRex and TMRrec	rs12143842	1	162033890		<i>C1orf226</i>	<i>UHMK1;SH2D1B</i>	<i>NOS1AP</i> (http://www.informatics.jax.org/marker/MGI:1917979); http://www.informatics.jax.org/marker/MGI:1341908)	<i>NOS1AP*</i>
<i>SCN5A-SCN10A</i>	TMRex and TMRrec	rs7373065 rs9311197 and rs7428232	3	38710315, 38776603 and 38778618	<i>SCN10A</i>		<i>SCN5A</i>	<i>SCN10A</i> (http://www.informatics.jax.org/marker/MGI:108029); http://www.informatics.jax.org/marker/MGI:98251)	<i>SCN5A, SCN10A</i>
<i>TSC22D2</i>	TMRrec	rs112717154	3	149943115			<i>EIF2A;TSC22D2</i>		<i>TSC22D2</i>
<i>CAMK2D</i>	TMRrec	rs35408611	4	114423677	<i>CAMK2D</i>			<i>CAMK2D</i> (http://www.informatics.jax.org/marker/MGI:1341265)	<i>CAMK2D</i>
<i>PREP</i>	TMRex	rs4478445	6	105786660	<i>PREP</i>		<i>ATG5;PREP</i>	<i>ATG5</i> (http://www.informatics.jax.org/marker/MGI:1270863); <i>PREP</i> (http://www.informatics.jax.org/marker/MGI:1277186)	<i>PREP, ATG5</i>
<i>KCNH2</i>	TMRex	rs2072412	7	150647970	<i>KCNH2</i>			<i>KCNH2</i> (http://www.informatics.jax.org/marker/MGI:1341722)	<i>KCNH2</i>
<i>KCNQ1</i>	TMRex and TMRrec	rs2074238	1	2484803	<i>KCNQ1</i>			<i>KCNQ1</i> (http://www.informatics.jax.org/marker/MGI:108083)	<i>KCNQ1</i>
<i>SOX5</i>	TMRex and TMRrec	rs7307613 and rs1396206	1 2	24595192 and 24576859	<i>SOX5</i>		<i>SOX5</i>		<i>SOX5</i>
<i>KLF12</i>	TMRrec	rs7992314	1 3	74509346	<i>KLF12</i>		<i>KLF12</i>		<i>KLF12</i>
<i>KCNJ2</i>	TMRex	17:68493468_GA_G	1 7	68493468			<i>CDC42EP4</i>	<i>CDC42EP4</i> (http://www.informatics.jax.org/marker/MGI:1929760)	<i>CDC42EP4</i>

*Abbreviations: SNV: Single-nucleotide variant, CHR: chromosome, BP: base pair position, based in HG build 18; eQTL: expression quantitative trait locus.

Column I provides URL links to mouse models with cardiovascular and neural phenotypes.

*NOS1AP** - this gene was selected as the likely candidate gene at this locus based on functional analyses and mouse models. *C1orf226* is a paralogue of *NOS1AP*.

The locus name indicates the coding gene that is in the closest proximity to the most associated SNV. The loci labelled as *TSC22D2* and *KCNJ2* have a lncRNA and a pseudogene as the nearest.

Supplemental Table 15. Candidate gene look-up for pleiotropy for cardiovascular diseases

Candidate gene(s)	Marker	GWAS catalogue		UKBiobank ICD PheWeb	
		Disease	P-value	Disease	P-value
<i>RNF207</i>	TMRex				
<i>SSBP3</i>	TMRrec				
<i>NOS1AP</i>	TMRex and TMRrec				
<i>SCN5A</i>	TMRex and TMRrec	Atrial fibrillation	3.00E-16	Atrial fibrillation and flutter	1.30E-08
	TMRex and TMRrec	Brugada syndrome	1.00E-14	First degree AV block	4.60E-08
<i>SCN10A</i>	TMRex and TMRrec	Brugada syndrome	1.00E-68	Atrial fibrillation and flutter	1.30E-08
	TMRex and TMRrec	Atrial fibrillation	2.00E-20		
<i>TSC22D2</i>	TMRrec	Cardiovascular disease	2.00E-13	Hypertension	1.10E-08
<i>CAMK2D</i>	TMRrec	Atrial fibrillation	2.00E-13		
<i>PREP</i>	TMRex				
<i>ATG5</i>	TMRex				
<i>KCNH2</i>	TMRex	Atrial fibrillation	2.00E-11	Hypertension	1.20E-25
	TMRex			Ischemic heart disease	2.70E-10
	TMRex			Myocardial infarction	9.20E-10
	TMRex			Coronary atherosclerosis	1.40E-08
<i>KCNQ1</i>	TMRex and TMRrec	Long QT	1.00E-54	Diabetes mellitus	2.40E-17
<i>SOX5</i>	TMRex and TMRrec	Atrial fibrillation	2.00E-17		
<i>KLF12</i>	TMRrec	Sudden cardiac arrest	5.00E-20		
<i>CDC42EP4</i>	TMRex				

Results are presented for all candidate genes for TMR during exercise or during recovery, with a genome-wide significant association with a cardiovascular or neural disease in GWASs published in the GWAS catalogue or the UK Biobank ICD PheWeb.

Supplemental Table 16: Net reclassification improvement for CV events with estimates of the expected number of reclassifications per risk category for cases and controls

Reclassification Table for all subjects

Standard	ESC SCORE + TMR during recovery ≥ 0.115				Reclassified up, n(%)	Reclassified down, n(%)	NRI (95% CI)
	< 1%	1 to <5%	5 to <10%	≥ 10%			
< 1%	4,167	145	0	0	738 (2.7)	794 (2.9)	0.019 (0.015- 0.022)
1 to <5%	173	16,366	298	0			
5 to <10%	0	368	4,633	295			
≥ 10%	0	0	253	799			

Reclassification Table for cases

Standard	ESC SCORE + TMR during recovery ≥ 0.115				Reclassified up, n(%)	Reclassified down, n(%)	NRI (95% CI)
	< 1%	1 to <5%	5 to <10%	≥ 10%			
< 1%	25	1	0	0	48 (5.7)	33 (3.9)	0.016 (0.012- 0.019)
1 to <5%	2	371	19	0			
5 to <10%	0	13	300	28			
≥ 10%	0	0	18	72			

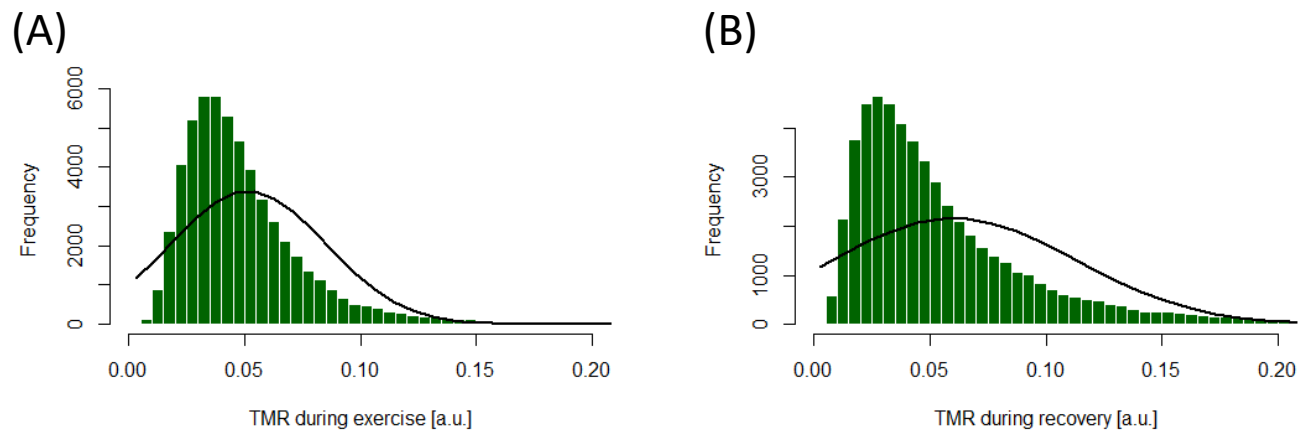
Reclassification Table for controls

Standard	ESC SCORE + TMR during recovery ≥ 0.115				Reclassified up, n(%)	Reclassified down, n(%)	NRI (95% CI)
	< 1%	1 to <5%	5 to <10%	≥ 10%			
< 1%	2,157	70	0	0	339 (2.6)	356 (2.7)	0.003 (0.002- 0.004)
1 to <5%	85	7,955	139	0			
5 to <10%	0	160	2,037	130			
≥ 10%	0	0	111	289			

ESC SCORE includes HTN, cholesterol, smoke, sex and age

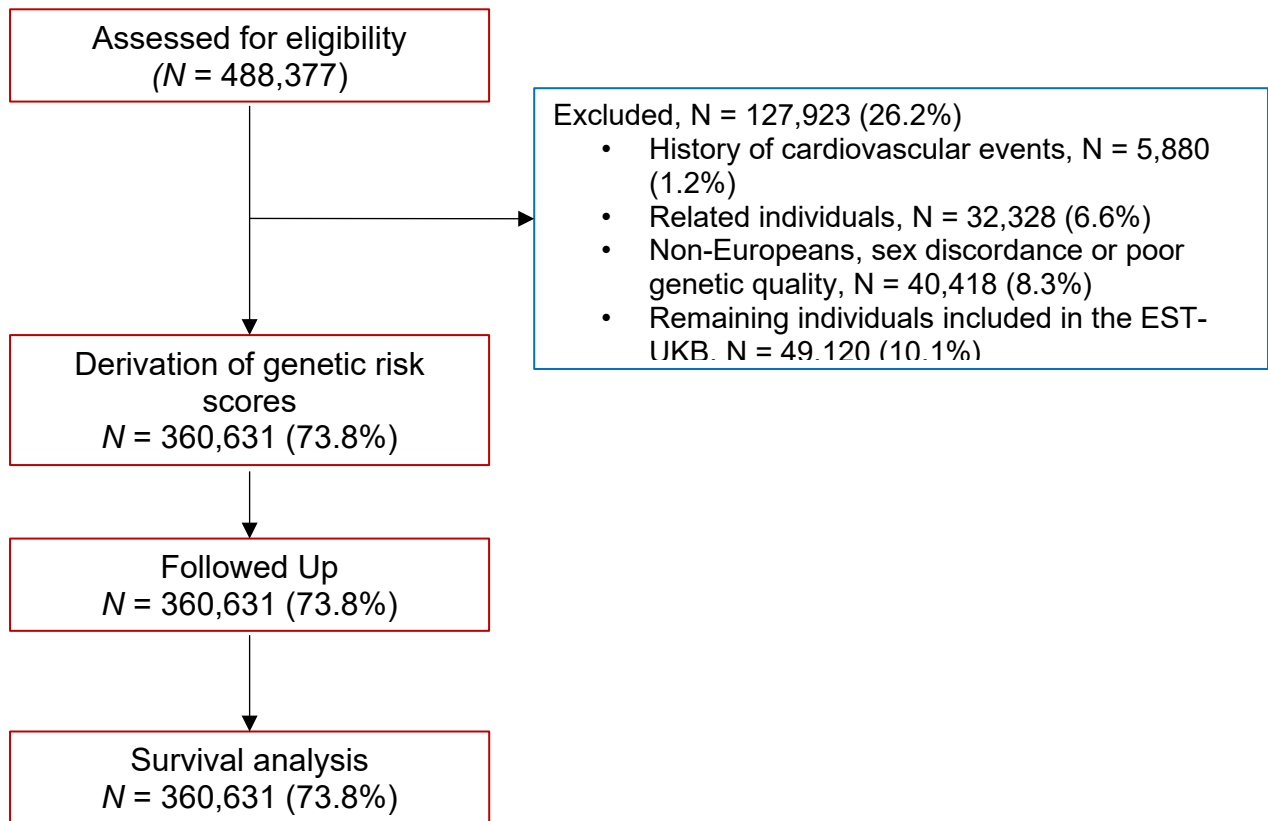
Abbreviations: ESC: European Society of Cardiology, TMR: T-wave morphology restitution, NRI: Net reclassification index, CI: confidence interval

Supplemental Figures

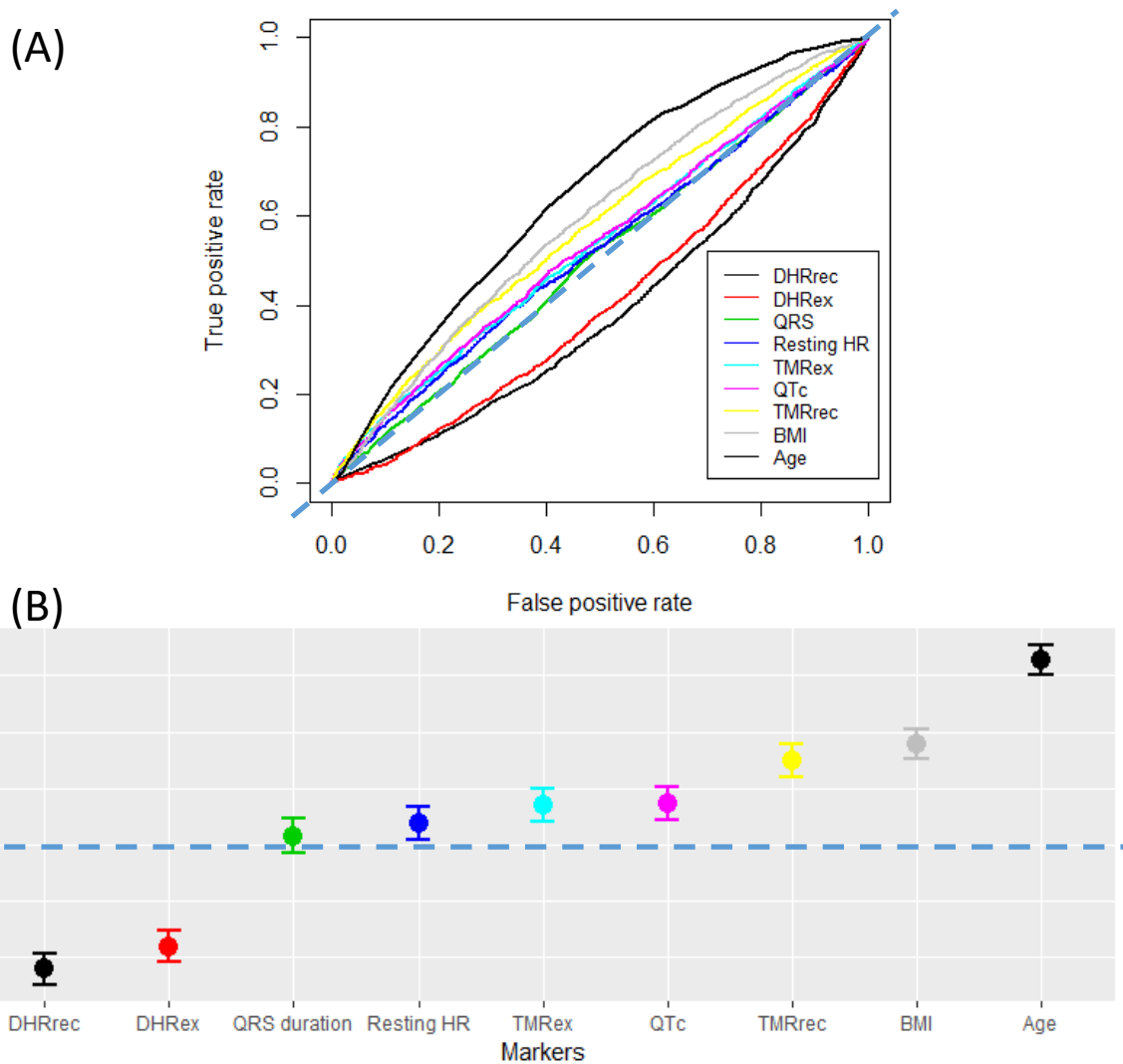


Supplemental Figure 1: Histograms of TMR during exercise (A) and TMR during recovery (B). The black curves indicate a normal distribution using the mean and standard deviation from each distribution.

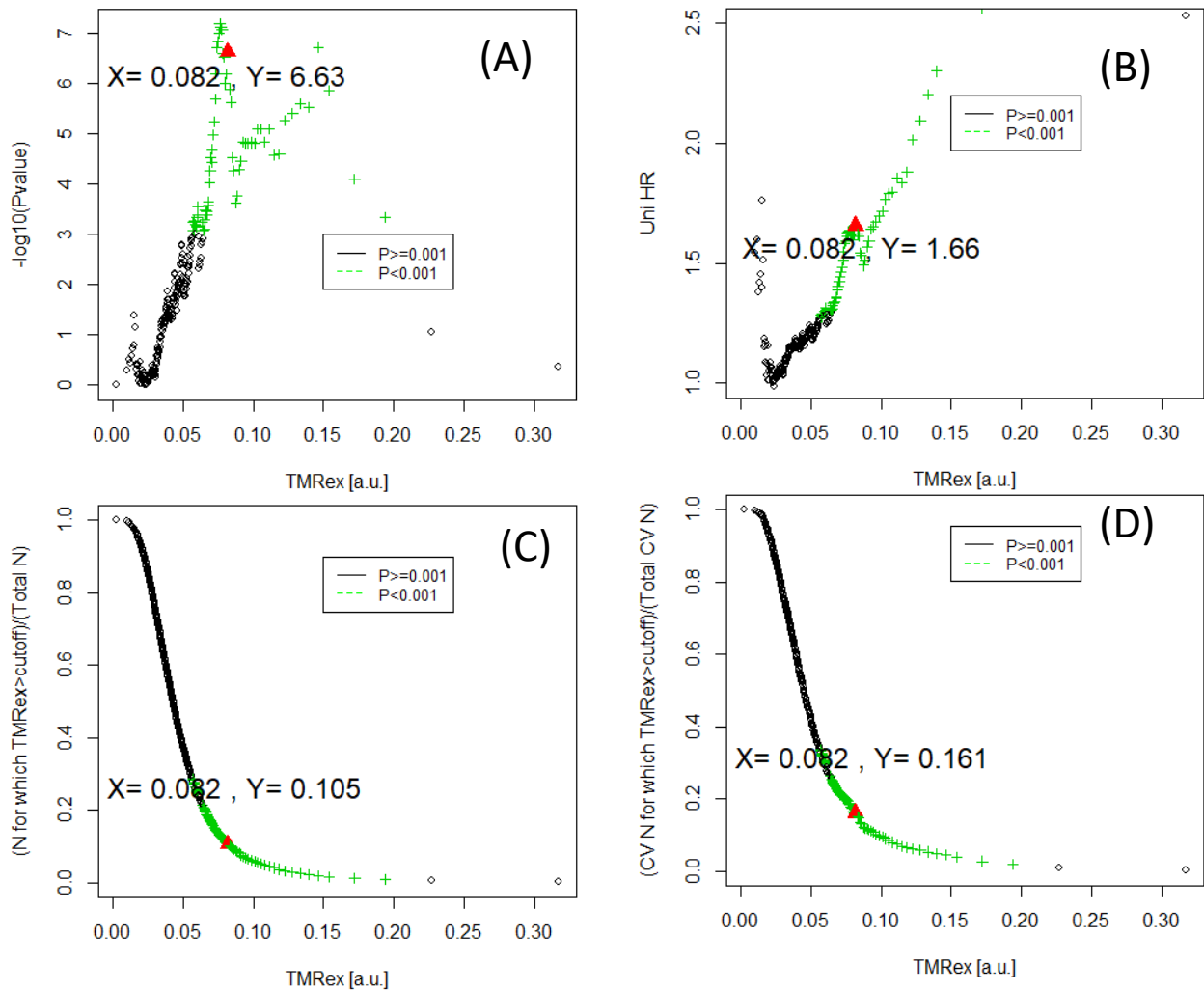
FULL-UKB cohort



Supplemental Figure 2: Full cohort (FULL-UKB) study population flow diagram.

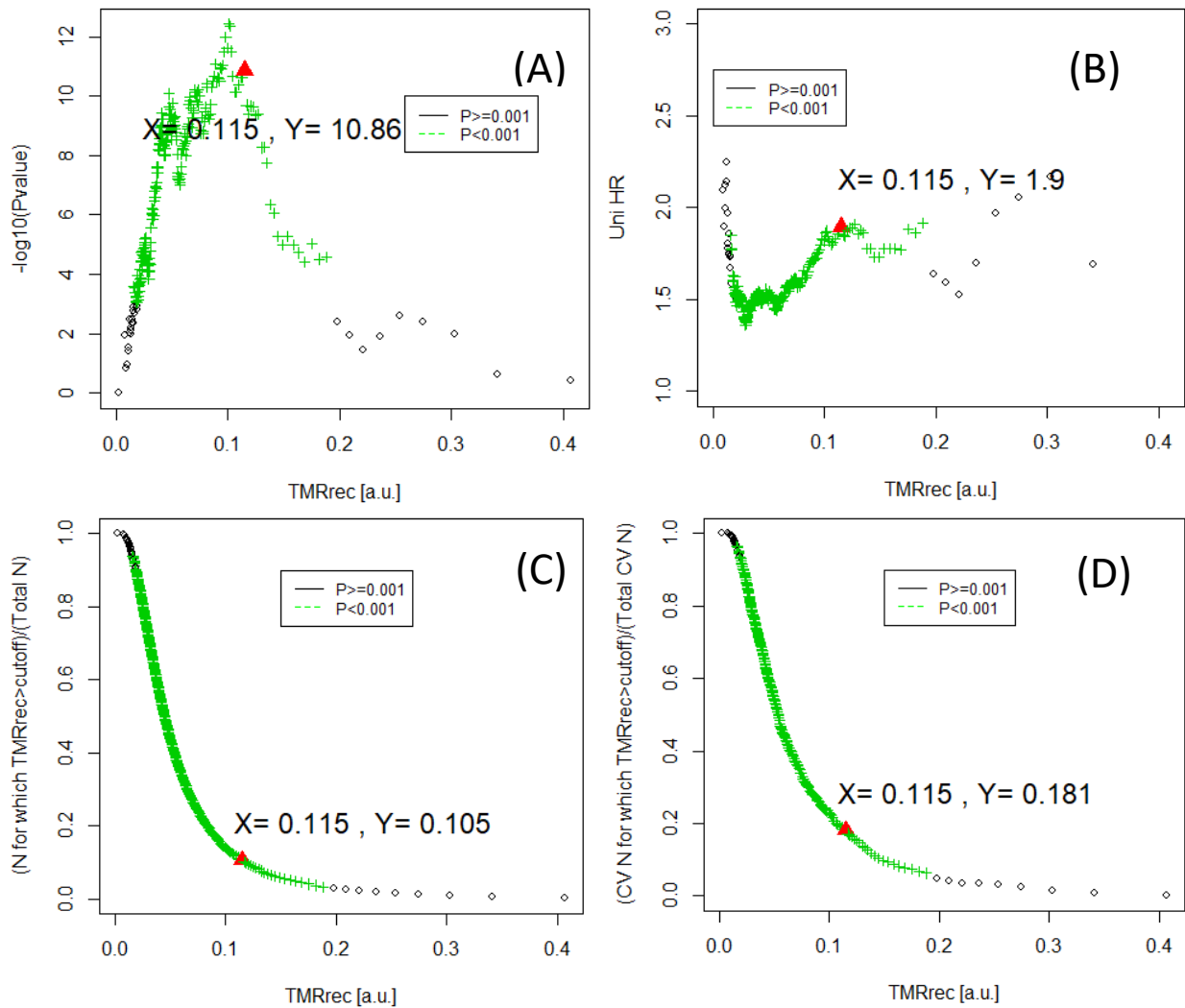


Supplemental Figure 3: Classification performance of clinical and ECG markers. (A) True positive rate versus false positive rate for the clinical and ECG markers, including TMR during exercise and recovery. (B) C-index for the clinical and ECG markers, including TMR during exercise and recovery. The dash-blue horizontal line indicates the C-index that would be obtained by chance.



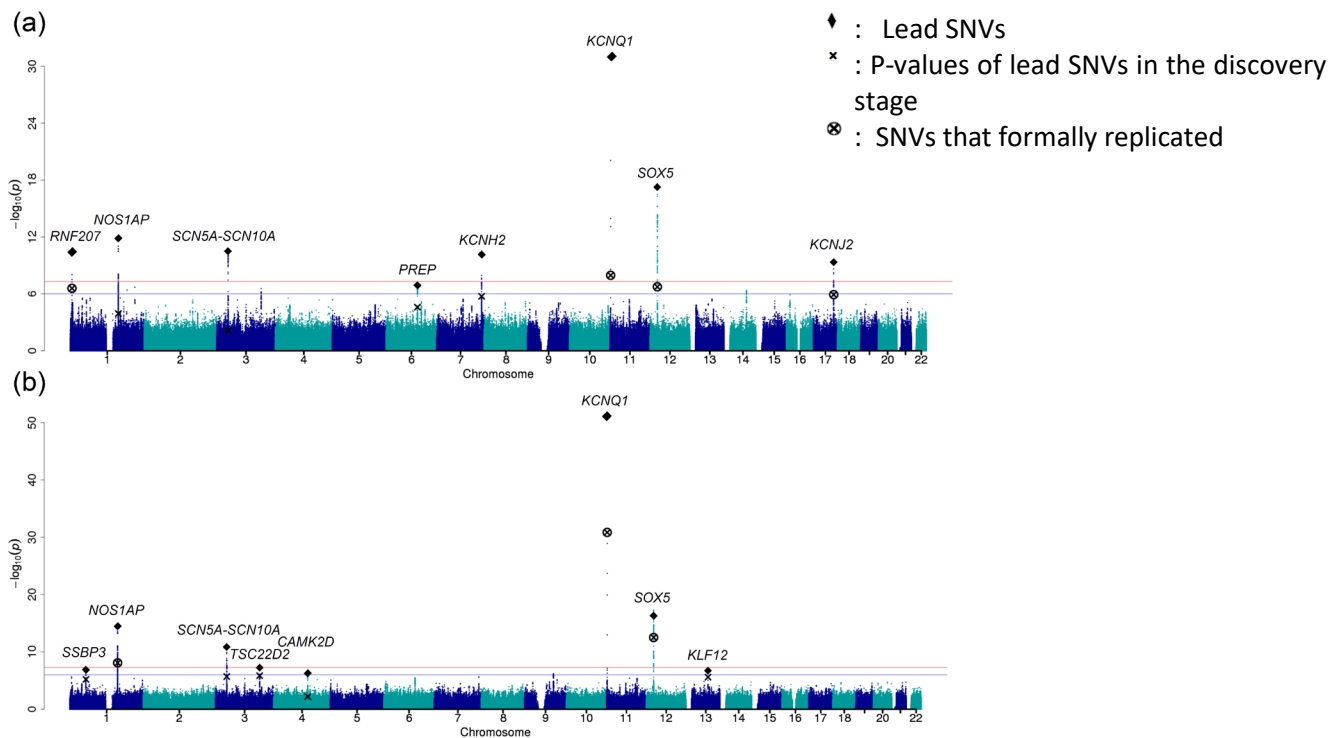
Supplemental Figure 4: Criteria to derive the optimal cut-off values for TMR during exercise.

A: $-\log_{10}(\text{P-value})$ versus TMR during exercise. B: Univariate hazard ratio (HR) versus TMR during exercise. C: Proportion of individuals with values of TMR during exercise above the cut-off vs TMR during exercise. D: Proportion of individuals from the CV event group with values of TMR during exercise above the cut-off vs TMR during exercise. The red triangle indicates the optimal cut-off value for TMR during exercise. The optimal cut-off value was defined as the one that simultaneously verified the following criteria: (i) it corresponded to a local maximum of the hazard ratio function from binary univariate Cox models, (ii) it was associated with a P -value $< 10^{-3}$ and (iii) the proportion of individuals in the high-risk and low-risk groups was $> 10\%$ and $> 50\%$, respectively. If more than one cut-off value met these criteria, the one associated with the highest hazard ratio was used.

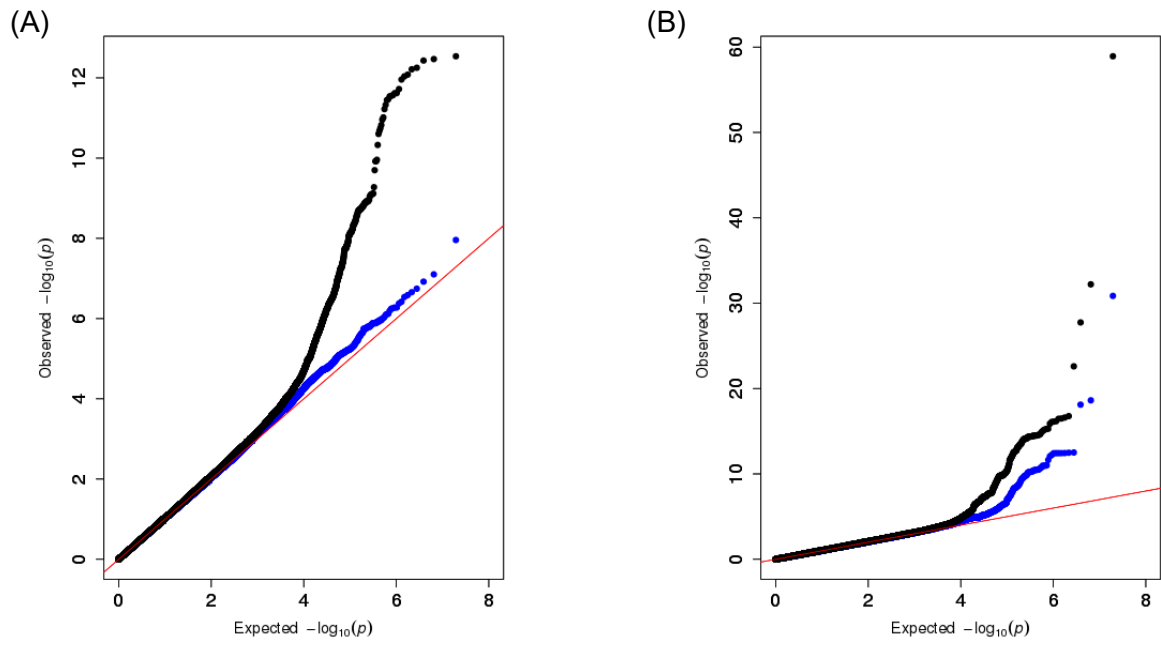


Supplemental Figure 5: Criteria to derive the optimal cut-off values for TMR during recovery.

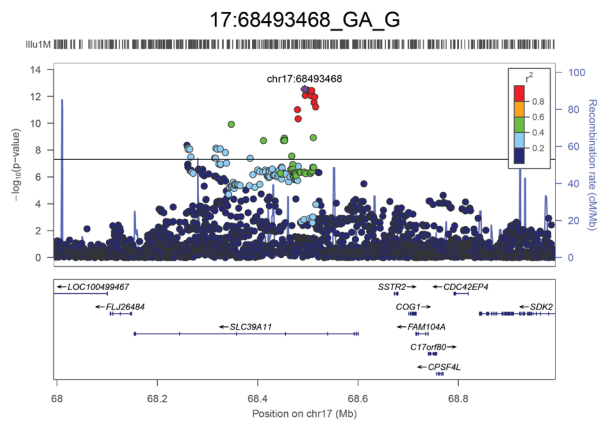
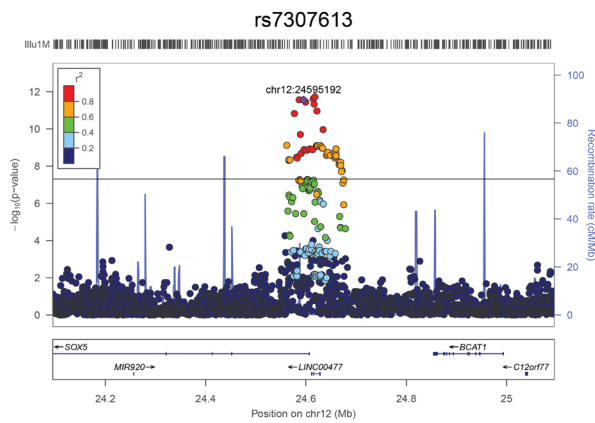
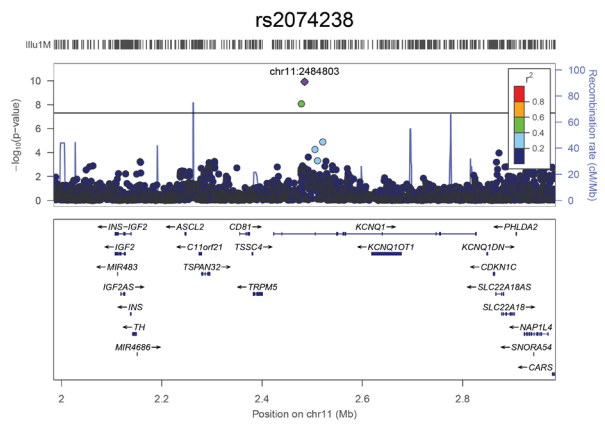
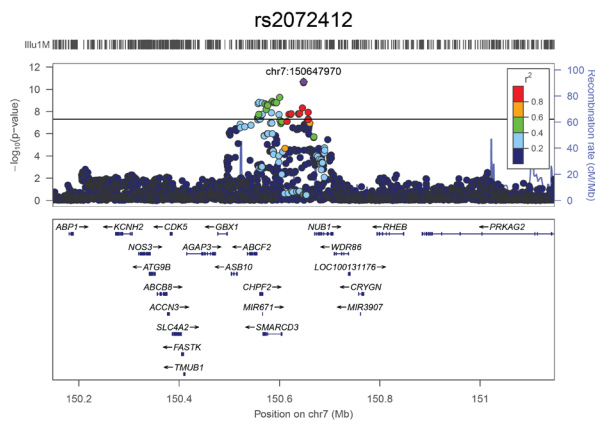
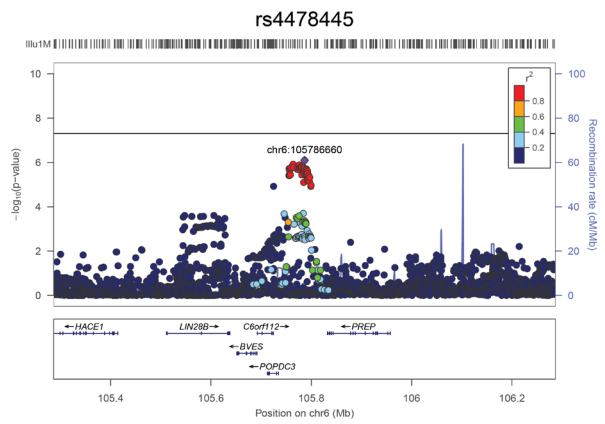
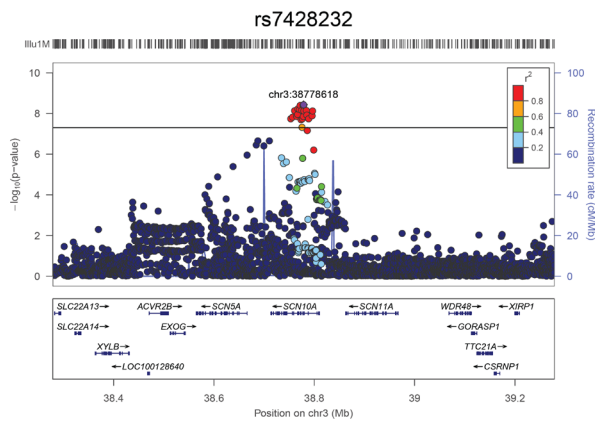
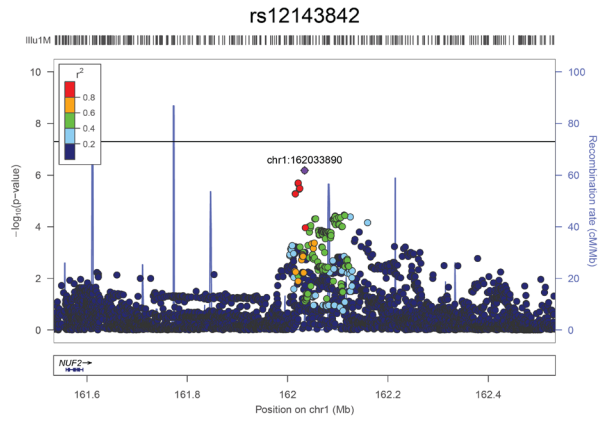
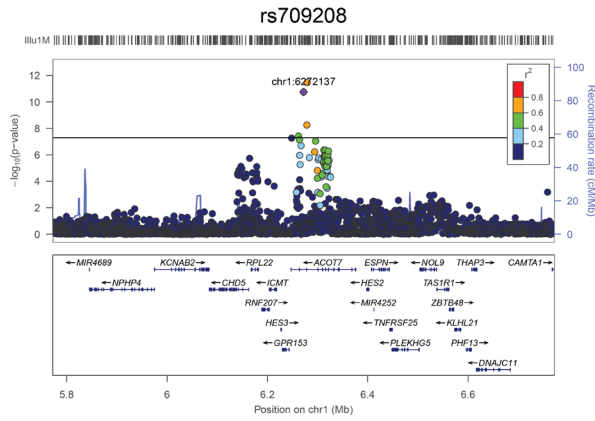
A: $-\log_{10}(\text{P-value})$ versus TMR during recovery. B: Univariate hazard ratio (HR) versus TMR during recovery. C: Proportion of individuals with values of TMR during recovery above the cut-off vs TMR during recovery. D: Proportion of individuals from the CV event group with values of TMR during recovery above the cut-off vs TMR during recovery. The red triangle indicates the optimal cut-off value for TMR during recovery. The optimal cut-off value was defined as the one that simultaneously verified the following criteria: (i) it corresponded to a local maximum of the hazard ratio function from binary univariate Cox models, (ii) it was associated with a P -value $< 10^{-3}$ and (iii) the proportion of individuals in the high-risk and low-risk groups was $> 10\%$ and $> 50\%$, respectively. If more than one cut-off value met these criteria, the one associated with the highest hazard ratio was used.



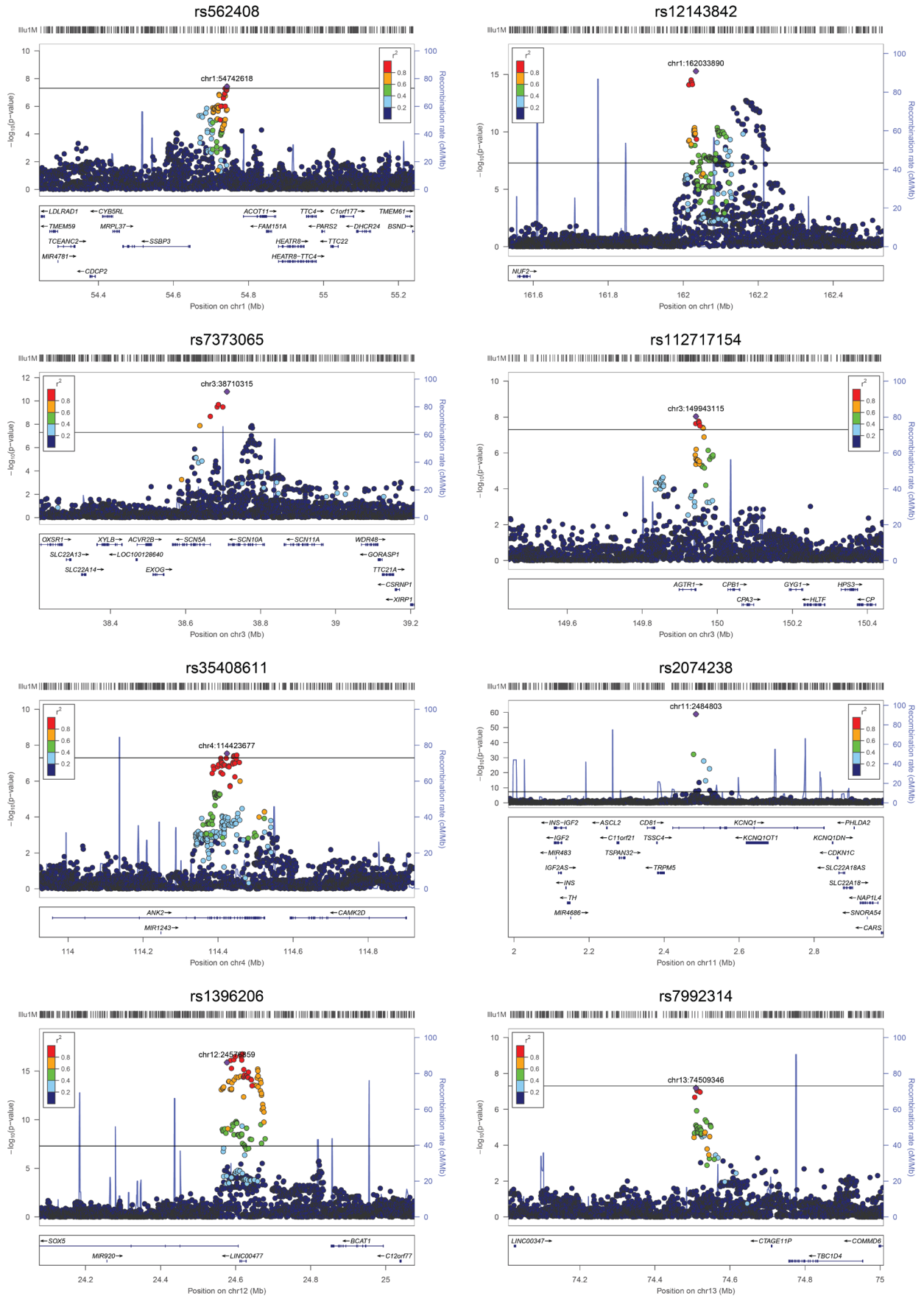
Supplemental Figure 6: Manhattan plots of TMR during exercise (a) and during recovery (b) in the full cohort analysis. P values, expressed as $-\log_{10}(P)$, are plotted according to physical genomic locations by chromosome. Lead SNVs are marked by the diamonds. The crosses indicate the P values of these SNVs in the discovery data set. Crosses are encircled for SNPs that formally replicated. Locus names of the novel loci correspond to the nearest annotated gene. The blue horizontal line indicates a P value threshold of 1×10^{-6} , corresponding to the lookup significance threshold. The red horizontal line indicates a P-value threshold of 5×10^{-8} , corresponding to genome-wide significance.



Supplemental Figure 7: QQ plots for TMR during exercise (A) and during recovery (B) in the discovery (blue) and full (black) cohorts.



Supplemental Figure 8A: Locus Zoom plots for all the identified loci for TMR during exercise.

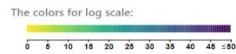


Supplemental Figure 8B: Locus Zoom plots for all the identified loci for TMR during recovery.

source	term name	term ID	n. of term genes	n. of query genes	n. of common genes	corrected p-value	CDR2EP4	SOX5	KONK1	KONK2	ATG5	PREP	SON10A	SON5A	NOS1AP	RNF207
BP	cardiac muscle cell action potential	GO:0086001	71	10	6	4.02e-10	M	S	M	M						
BP	regulation of ventricular cardiac muscle cell membrane repolarization	GO:0060307	24	10	5	4.69e-10	M	M	M							
BP	ventricular cardiac muscle cell membrane repolarization	GO:0099625	28	10	5	1.08e-09	M	M	M							
BP	regulation of cardiac muscle cell membrane repolarization	GO:0099623	29	10	5	1.31e-09	M	M	M							
BP	ventricular cardiac muscle cell action potential	GO:0086005	36	10	5	4.15e-09	M	S	M							
BP	regulation of membrane repolarization	GO:0060306	37	10	5	4.79e-09	M	M	M							
BP	heart contraction	GO:0060047	245	10	7	5.44e-09	M	M	M		e					
BP	cardiac muscle cell membrane repolarization	GO:0099622	39	10	5	6.33e-09	M	M	M							
BP	heart process	GO:0003015	253	10	7	6.82e-09	M	M	M		e					
BP	membrane repolarization	GO:0086009	48	10	5	1.88e-08	M	M	M							

The colors for different evidence codes in the table:

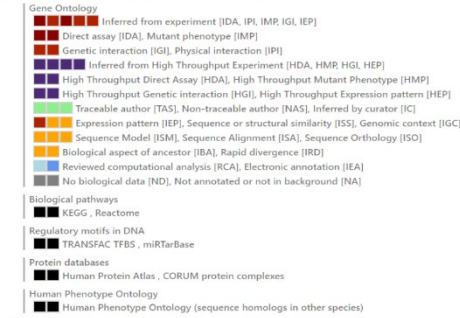
- Gene Ontology
 - Inferred from experiment [IDA, IPI, IMP, IGI, IEP]
 - Direct assay [IDA], Mutant phenotype [IMP]
 - Genetic interaction [IGI], Physical interaction [IPI]
 - Inferred from High Throughput Experiment [HDA, HMR, HGI, HEP]
 - High Throughput Direct Assay [HDA], High Throughput Mutant Phenotype [HMP]
 - High Throughput Genetic Interaction [HGI], High Throughput Expression pattern [HEP]
 - Traceable author [TAS], Non-traceable author [NAS], Inferred by curator [IC]
 - Expression pattern [IEP], Sequence or structural similarity [ISS], Genomic context [IGC]
 - Sequence Model [ISM], Sequence Alignment [ISA], Sequence Orthology [ISO]
 - Biological aspect of ancestor [IBA], Rapid divergence [IRD]
 - Reviewed computational analysis [RCA], Electronic annotation [IEA]
 - No biological data [ND], Not annotated or not in background [NA]
- Biological pathways
 - KEGG, Reactome
- Regulatory motifs in DNA
 - TRANSFAC, TFBS, miRTarBase
- Protein databases
 - Human Protein Atlas, CORUM protein complexes
- Human Phenotype Ontology
 - Human Phenotype Ontology (sequence homologs in other species)



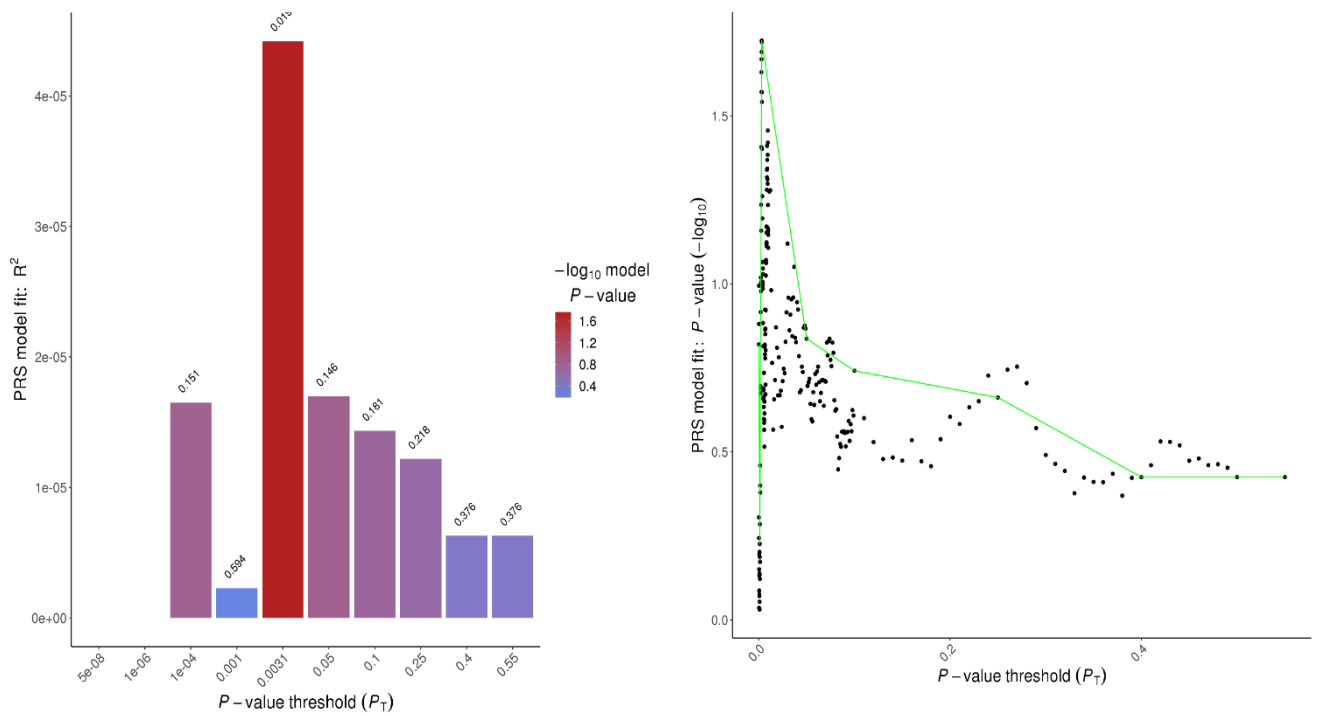
Supplemental Figure 9: Biological processes enrichment of candidate genes at TMR during exercise loci. g:profiler GO (gene ontology) term enrichment was performed using the candidate genes for TMR during exercise.

source	term name	term ID	n. of term genes	n. of query genes	n. of common genes	corrected p-value	KLF12	SOX5	KONQ1	GMK2D	TSC2D2	SCN10A	SCN5A	NOST1AP	SSBP3
BP	cardiac muscle cell action potential	G0:0086001	71	9	5	6.60e-08	S	M	M	S	M				
BP	regulation of cardiac muscle contraction	G0:0055117	80	9	5	1.22e-07	S	M	M	S	M				
BP	regulation of striated muscle contraction	G0:0006942	95	9	5	2.92e-07	S	M	M	S	M				
BP	regulation of heart rate	G0:0002027	100	9	5	3.80e-07	H	M	M	C	M				
rea	Cardiac conduction	R-HSA-5576891	137	4	4	1.05e-06	r	r	r	r	r				
BP	cardiac muscle contraction	G0:0060048	134	9	5	1.67e-06	S	M	M	S	M				
BP	action potential	G0:0001508	142	9	5	2.24e-06	S	D	M	S	D				
rea	Muscle contraction	R-HSA-397014	200	4	4	4.84e-06	r	r	r	r	r				
BP	regulation of muscle contraction	G0:0006937	168	9	5	5.24e-06	S	M	M	S	M				
BP	cell communication involved in cardiac conduction	G0:0086065	54	9	4	6.26e-06	H	M	C	M					

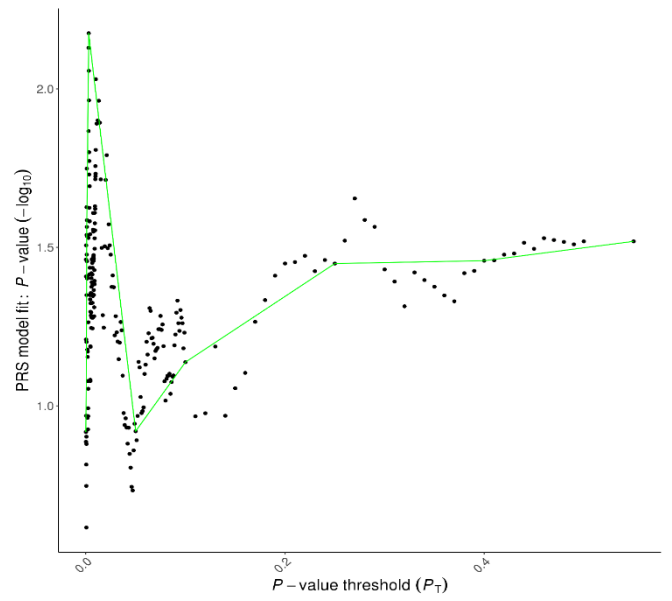
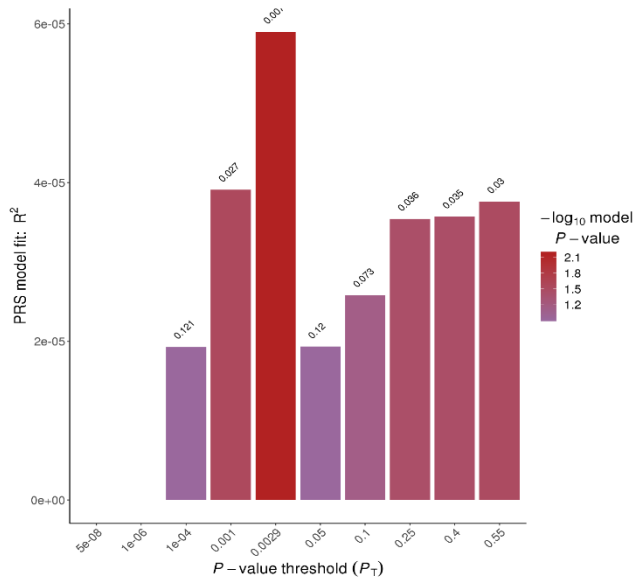
The colors for different evidence codes in the table:



Supplemental Figure 10: Biological processes enrichment of candidate genes at TMR during recovery loci. g:profiler GO (gene ontology) term enrichment was performed using the candidate genes for TMR during recovery.



Supplemental Figure 11: Left, adjusted R-squared versus the P-value threshold. Right, -log₁₀ of the P-value from each logistic regression versus the P-value threshold. The optimal P-value threshold is the one for which the adjusted R-squared is highest and the P-value is lowest.



Supplemental Figure 12: Left, adjusted R-squared versus the P-value threshold. Right, $-\log_{10}$ of the P-value from each logistic regression versus the P-value threshold. The optimal P-value threshold is the one for which the adjusted R-squared is highest and the P-value is lowest.

Supplemental References

1. Orini M, Tinker A, Munroe PB and Lambiase PD. Long-term intra-individual reproducibility of heart rate dynamics during exercise and recovery in the UK Biobank cohort. *PLOS ONE*. 2017;12:e0183732.
2. Ramírez J, Duijvenboden Sv, Ntalla I, Mifsud B, Warren HR, Tzanis E, Orini M, Tinker A, Lambiase PD and Munroe PB. Thirty loci identified for heart rate response to exercise and recovery implicate autonomic nervous system. *Nature Communications*. 2018;9:1947.
3. Bazett HC. An Analysis of the Time-Relations of Electrocardiograms. *Annals of Noninvasive Electrocardiology*. 1997;2:177-194.
4. Saito T and Rehmsmeier M. The Precision-Recall Plot Is More Informative than the ROC Plot When Evaluating Binary Classifiers on Imbalanced Datasets. *PLOS ONE*. 2015;10:e0118432.
5. Steger A, Müller A, Barthel P, Dommasch M, Huster KM, Hnatkova K, Sinnecker D, Hapfelmeier A, Malik M and Schmidt G. Polyscore of Non-invasive Cardiac Risk Factors. *Frontiers in Physiology*. 2019;10.
6. Pencina MJ, D'Agostino Sr RB and Steyerberg EW. Extensions of net reclassification improvement calculations to measure usefulness of new biomarkers. *Statistics in Medicine*. 2011;30:11-21.
7. Piepoli MF, Hoes AW, Agewall S, Albus C, Brotons C, Catapano AL, Cooney M-T, Corrà U, Cosyns B, Deaton C, Graham I, Hall MS, Hobbs FDR, Løchen M-L, Löllgen H, Marques-Vidal P, Perk J, Prescott E, Redon J, Richter DJ, Sattar N, Smulders Y, Tiberi M, van der Worp HB, van Dis I, Verschuren WMM, Binno S and Group ESD. 2016 European Guidelines on cardiovascular disease prevention in clinical practice: The Sixth Joint Task Force of the European Society of Cardiology and Other Societies on Cardiovascular Disease Prevention in Clinical Practice (constituted by representatives of 10 societies and by invited experts) Developed with the special contribution of the European Association for Cardiovascular Prevention & Rehabilitation (EACPR). *European Heart Journal*. 2016;37:2315-2381.
8. Bycroft C, Freeman C, Petkova D, Band G, Elliott LT, Sharp K, Motyer A, Vukcevic D, Delaneau O, O'Connell J, Cortes A, Welsh S, McVean G, Leslie S, Donnelly P and Marchini J. Genome-wide genetic data on ~500,000 UK Biobank participants. *bioRxiv*. 2017.
9. Chang CC, Chow CC, Tellier LCAM, Vattikuti S, Purcell SM and Lee JJ. Second-generation PLINK: rising to the challenge of larger and richer datasets. *GigaScience*. 2015;4:1-16.
10. Ramírez J, van Duijvenboden S, Ntalla I, Mifsud B, Warren HR, Tzanis E, Orini M, Tinker A, Lambiase PD and Munroe PB. Thirty loci identified for heart rate response to exercise and recovery implicate autonomic nervous system. *Nature communications*. 2018;9:1947.
11. Loh P-R, Bhatia G, Gusev A, Finucane H, Bulik-Sullivan B, Pollack S, Group P-SW, de Candia T, Lee S, Wray N, Kendler K, O'Donovan M, Neale B, Patterson N and Price A. Contrasting genetic architectures of schizophrenia and other complex diseases using fast variance components analysis. *Nature Genetics*. 2015;47:1385-1392.
12. Loh P-R, Tucker G, Bulik-Sullivan B, Vilhjalmsson B, Finucane H, Salem R, Chasman D, Ridker P, Neale B, Berger B, Patterson N and Price A. Efficient Bayesian mixed model analysis increases association power in large cohorts. *Nature Genetics*. 2015;47:284-290.
13. Turley P, Walters RK, Maghazian O, Okbay A, Lee JJ, Fontana MA, Nguyen-Viet TA, Wedow R, Zacher M, Furlotte NA, Magnusson P, Oskarsson S, Johannesson M, Visscher PM, Laibson D, Cesarini D, Neale BM, Benjamin DJ, Agee M, Alipanahi B, Auton A, Bell RK, Bryc K, Elson SL, Fontanillas P, Furlotte NA, Hinds DA, Hromatka BS, Huber KE, Kleinman A, Litterman NK, McIntyre MH, Mountain JL, Northover CAM, Sathirapongsasuti JF, Sazonova OV, Shelton JF, Shringarpure S, Tian C, Tung JY, Vacic V, Wilson CH, Pitts SJ, and Me Research T and Social Science Genetic Association C. Multi-trait analysis of genome-wide association summary statistics using MTAG. *Nature Genetics*. 2018;50:229-237.

14. Staley JR, Blackshaw J, Kamat MA, Ellis S, Surendran P, Sun BB, Paul DS, Freitag D, Burgess S, Danesh J, Young R and Butterworth AS. PhenoScanner: a database of human genotype–phenotype associations. *Bioinformatics*. 2016;32:3207-3209.
15. McLaren W, Gil L, Hunt SE, Riat HS, Ritchie GRS, Thormann A, Flicek P and Cunningham F. The Ensembl Variant Effect Predictor. *Genome Biology*. 2016;17:122.
16. Boyle AP, Hong EL, Hariharan M, Cheng Y, Schaub MA, Kasowski M, Karczewski KJ, Park J, Hitz BC, Weng S, Cherry JM and Snyder M. Annotation of functional variation in personal genomes using RegulomeDB. *Genome Research*. 2012;22:1790-1797.
17. Raudvere U, Kolberg L, Kuzmin I, Arak T, Adler P, Peterson H and Vilo J. g:Profiler: a web server for functional enrichment analysis and conversions of gene lists (2019 update). *Nucleic Acids Research*. 2019.
18. Dickinson ME, Flenniken AM, Ji X, Teboul L, Wong MD, White JK, Meehan TF, Wenginger WJ, Westerberg H, Adissu H, Baker CN, Bower L, Brown JM, Caddle LB, Chiani F, Clary D, Cleak J, Daly MJ, Denegre JM, Doe B, Dolan ME, Edie SM, Fuchs H, Gailus-Durner V, Galli A, Gambadoro A, Gallegos J, Guo S, Horner NR, Hsu C-W, Johnson SJ, Kalaga S, Keith LC, Lanoue L, Lawson TN, Lek M, Mark M, Marschall S, Mason J, McElwee ML, Newbigging S, Nutter LMJ, Peterson KA, Ramirez-Solis R, Rowland DJ, Ryder E, Samocha KE, Seavitt JR, Selloum M, Szoke-Kovacs Z, Tamura M, Trainor AG, Tudose I, Wakana S, Warren J, Wendling O, West DB, Wong L, Yoshiki A, The International Mouse Phenotyping C, McKay M, Urban B, Lund C, Froeter E, LaCasse T, Mehalow A, Gordon E, Donahue LR, Taft R, Kutney P, Dion S, Goodwin L, Kales S, Urban R, Palmer K, Pertuy F, Bitz D, Weber B, Goetz-Reiner P, Jacobs H, Le Marchand E, El Amri A, El Fertak L, Ennah H, Ali-Hadji D, Ayadi A, Wattenhofer-Donze M, Jacquot S, André P, Birling M-C, Pavlovic G, Sorg T, Morse I, Benso F, Stewart ME, Copley C, Harrison J, Joynson S, Guo R, Qu D, Spring S, Yu L, Ellegood J, Morikawa L, Shang X, Feugas P, Creighton A, Castellanos Penton P, Danisment O, Griggs N, Tudor CL, Green AL, Icoresi Mazzeo C, Siragher E, Lillistone C, Tuck E, Gleeson D, Sethi D, Bayzatinova T, Burvill J, Habib B, Weavers L, Maswood R, Miklejewska E, Woods M, Grau E, Newman S, Sinclair C, Brown E, Ayabe S, Iwama M, Murakami A, Wurst W, MacArthur DG, Tocchini-Valentini GP, Gao X, Flicek P, Bradley A, Skarnes WC, Justice MJ, Parkinson HE, Moore M, Wells S, Braun RE, Svenson KL, de Angelis MH, Herault Y, Mohun T, Mallon A-M, Henkelman RM, Brown SDM, Adams DJ, Lloyd KCK, McKelvie C, Beaudet AL, Bućan M and Murray SA. High-throughput discovery of novel developmental phenotypes. *Nature*. 2016;537:508.
19. Smith CL, Blake JA, Kadin JA, Richardson JE, Bult CJ and the Mouse Genome Database G. Mouse Genome Database (MGD)-2018: knowledgebase for the laboratory mouse. *Nucleic Acids Research*. 2018;46:D836-D842.
20. Buniello A, MacArthur JA L, Cerezo M, Harris LW, Hayhurst J, Malangone C, McMahon A, Morales J, Mountjoy E, Sollis E, Suveges D, Vrousitou O, Whetzel PL, Amode R, Guillen JA, Riat HS, Trevanion SJ, Hall P, Junkins H, Flicek P, Burdett T, Hindorf LA, Cunningham F and Parkinson H. The NHGRI-EBI GWAS Catalog of published genome-wide association studies, targeted arrays and summary statistics 2019. *Nucleic Acids Research*. 2018;47:D1005-D1012.